Accurately Identifying Functional Flow Metrics in Flashy and Highly Altered Stream Systems

By

CAMERON J CARPENTER
THESIS

Submitted in partial satisfaction of the requirements for the degree of

MASTER OF SCIENCES

in

Civil & Environmental Engineering

in the

OFFICE OF GRADUATE STUDIES

of the

UNIVERSITY OF CALIFORNIA

DAVIS

Approved:

_____

Jay Lund, Chair

_____

Sarah Yarnell

_____

Jon Herman

Committee in Charge

2024

Identifying Functional Flow Metrics in Flashy and Highly Altered Stream Systems

By Cameron Carpenter, Center for Watershed Sciences, UC Davis

Abstract

The unique Mediterranean climate and geography of California contributes to predictable flow patterns in its rivers, enabling researchers to discern key hydrologic metrics indicative of stream health for diverse species. The California Environmental Flows Working Group (CEFWG) introduced the California Environmental Flows Framework (CEFF) in 2021 to provide a holistic approach to analyze environmental flows throughout the diverse state. CEFF identifies five functional flow components described by 23 functional flow metrics that capture historical environmental functionality. However, challenges arise when applying these metrics to less predictable flashy streams or highly altered river systems, such as those impacted by dams or diversions, resulting in inaccurate assessments. The alterations to California's hydrology through dam construction, water transfers, and reservoir management have significantly modified natural flow regimes, affecting downstream ecosystems and native species like salmon. Improved management of streamflow is crucial for sustainable water use and the preservation of native ecosystems.

To address these challenges, the Functional Flow Calculator - Flashy (FFC-F) was developed to accurately calculate functional flow metrics in naturally flashy streams and highly altered systems. Unlike the original reference-based Functional Flow Calculator (FFC-R), which performs well in streams with natural predictable seasonal flows but struggles with accurate

assessments in highly altered systems, the FFC-F minimizes data smoothing and relies on abrupt changes in flow to identify seasonal transitions. Through an alternate functional flow identification algorithm, the FFC-F targets rapid rates of change or flat-lined flows, common in altered basins or less predictable rain-driven streams. By eliminating extensive data filtering, the FFC-F captures the nuanced flow dynamics characteristic of these systems, offering a more accurate representation of functional flow components. The FFC-F thus provides a valuable complementary tool within CEFF for regulators, planners, and dam operators to navigate the complexities of managing environmental flows in a rapidly evolving hydrological landscape.

Table of Contents

1 Introduction 1

2 METHODS 4

2.1 Study Area 4

2.2 Study Data 5

2.3 Alternate Function Flow Identification Algorithm Development 6

2.3.1 Spring Recession 6

2.3.2 Dry Season 10

2.3.3 Fall Pulse 14

2.3.4 Wet Season Baseflow 16

2.3.5 Peak Flow Prediction 19

3 Results 21

3.1 Functional Flow Calculator – Flashy Performance 22

3.2 Functional Flow Calculator Comparison 24

3.2.1 Flashy Ephemeral Rain-Driven Systems 27

3.2.2 Highly Altered Systems 33

4 Calculator Selection 35

5 Case Studies 42

5.1 Sacramento River Near Keswick Dam 42

5.2 Salinas River near Pozo California 46

6 Conclusion 51

7 References 54

Appendix A: Gage Data 58

Table of Figures

Figure 1: Five functional flow components (boxes) used to describe the flow regimes typical of California rivers. These five components can be quantified through flow characteristics/metrics shown the table (Yarnell et al. 2020). 2

Figure 2: Visualization of Spring Recession Start Timing Identification For FFC-R Rule Set: (a) A wide Gaussian filter is applied to the raw flow data. (b) The global maximum for that water year is found in the filtered data and a timing window is set from 20 days before until 50 days after the global maximum. (c) Within the timing window, a narrow Gaussian Filter is applied. (d) Peaks are identified and the last peak above the 50th percentile of narrowly filtered data that meets the slope threshold is identified as the spring recession start (Appendix C CEFWG 2021). 8

Figure 3: Visualization of Spring Recession Start Timing Identification For FFC-F Rule Set: (1) The Raw flow data for the water year is smoothed using a narrow Gaussian filter. (2) Peaks in

the smoothed data are identified. (3) Look backward from the end of the year to find the last peak above the 90th percentile of flow that water year in the smoothed data. (4) The day with maximum flow within 4 days of the peak identified in the smoothed data is selected as the spring recession start date. 9
Figure 4: Visualization of Dry Season Start Timing Identification For FFC-F Rule Set: (1) The raw flow data and previously calculated spring recession are loaded in. (2) The dry season start threshold is set using Equation 1. (3) Going forward from the start of the spring recession each day is tested to see if it meets the dry season start criteria. (4) Once there are five consecutive days meeting the dry season start criteria then the dry season start is selected. 13
Figure 5: Visualization Fall Pulse Timing Identification For FFC-F Rule Set: (1) The previous dry season start timing and raw flow data for the previous and current water year is loaded. (2) The flow data after the previous dry season start has a running median taken, which is then multiplied by 1.5 for the threshold for the fall pulse to occur. (3) Peaks are identified between October 1st and December 15th of the current water year. The first peak above the threshold is selected as the fall pulse for the current water year. 15
Figure 6: Visualization Wet Season Timing Identification For FFC-F Rule Set: (1) The raw flow data and the fall pulse are loaded in. (2) The rolling median of the flow data after the fall pulse is compared to that same value multiplied by one and a half to set the threshold for the wet season starting. (3) the wet season is selected as the first day above the threshold. 18
Figure 7: In a reference FER stream (USGS gage ID: 11120510, San Jose Creak at Goleta, CA) in Water Year 1988. (1) A fall pulse is detected by FFC-F when a storm event causes a return flow over the fall threshold (olive dashed line). (2) FFC-F then looks forward until there is a day with flow equal or greater than one and a half times the running median of flow after the fall pulse. (3) FFC-R uses the smoothed data to set a flow and slope threshold. (4) FFC-R then looks backwards until both are met in this case the slope threshold (not shown) is not met until near the beginning of the water year. The wet season timing is so early that FFC-R does not count the fall pulse that occurs. In this case FFC-F more accurately predicts the wet season start and identifies an accurate fall pulse that FFC-R does not. 29
Figure 8: Calculator Dry season start comparison at USGS gage 11138500 (Sisquoc River Near Sisquoc, CA), and FER reference gage, during water year 1960. (1) One large peak during the wet season set a higher dry season start threshold [light green line]. (2/3) The smoothed data reduces peak in the wet season by approximately an order of magnitude (~250 cfs to ~25 cfs), which in turn sets a low flow threshold and slope threshold in FFC-R. This low threshold means that it takes a long time for both flow data to satisfy both thresholds even though flow had been practically flatlined for months. 31
Figure 9: Metrics with significant differences between the FFC-F and FFC-R in FER Systems 32
Figure 10: Metrics with significant differences between the FFC-F and FFC-R in Highly Altered Systems 34
Figure 11: Average number of NA's produced by the FFC-R for each stream class reference gage and highly altered gage. There is a break in interquartile ranges of the reference gages compared to the FER gage and highly altered gages around 0.5 and 0.7. 37
Figure 12: RBFI calculated using all flow data across stream classes and in highly altered streams. 39
Figure 13: A Comparison of the annual average NAs produced by FFC-R summed with RBFI across stream classes. 40

Figure 14: Monthly mean full natural flow rate (blue) and monthly mean observed flow (orange) on the Sacramento River below Shasta Dam. Full natural flow from California Data Exchange Center (CDEC) site Sacto Inflow-Shasta ('SIS') and mean observed flow from CDEC site Shasta Dam ('SHA). Box plots indicate the historical variability for each month. 43
Figure 15: A comparison of FNF (green) and overserved flow (blue) in the Sacramento River around Shasta Reservoir in an above normal year (WY 2000) and a dry year (WY 2001). 44
Figure 16: Natural ranges of function flow metrics for the Sacramento River below Keswick Dam compared to the observed median values (Grantham et al. 2022). Values in green are considered unaltered and values in red are considered likely altered (CEFWG 2021). 45
Figure 17: A comparison of the natural range of function flow metrics predicted for the reference gage 11143500 - Salinas River near Pozo California (1) and gage 11144600 - Salinas River Below Salinas Dam (2). 47
Figure 18: Functional Flow Metrics Calculated by the FFC-R for Salinas River near Pozo California. In water years 1974 and 1975, the dry season start is months after the flow has flatlined. In 1974 and 1976, the wet season start is identified while flow is still relatively flat before base flows increased. 48
Figure 19: Comparing Flows from Reference Gage 11143500: Salinas River Near Pozo and gage 11144600: Salinas River below Salinas Dam for water year 1979. 49
Figure 20: Comparing environmental flow regimes produced based on the FFC-F and the FFC-R and to the observed flow for Water Year 1966. 50
Figure 21: Functional flow metric to annual flow volume percentile relationships. The relationship in red is proposed in Murdoch 2024, and the relationship in green is a potentially more accurate piecewise function also discussed in Murdoch 2024. 51

Table of Tables

Table 1: Issues in Timing Observed in the FFC-F For Flashy Ephemeral Streams and Highly Altered Streams 23
Table 2: Difference between timing metrics for the FFC-R and FFC-F in two sets of gages (FER and highly altered streams) using criteria based on the number of days of difference in timing . 26
Table 3: Calculator Rule Set Selection Testing 41
Table 4: Calculator Rule Set Selection Validation 41

1 Introduction

California's Mediterranean climate and geography result in unusually predictable stream flow patterns in its rivers (Gasith and Resh 1999). This predictability has allowed researchers to analyze annual hydrographs and identify key metrics in the flow regimes that relate to a healthy stream environment for native aquatic species (CEFWG 2021). Many studies propose flow metrics for various environments, ecosystems, and species. As of 2003, over 200 methods have been proposed for determining environmental flows, with additional new methods published since (Tharme 2003; Arthington et al. 2018; Williams et al. 2019). One newer approach was published by the California Environmental Flows Working Group (CEFWG) in 2021 proposing a holistic method for analyzing environmental flows in California called the California Environmental Flows Framework (CEFF). This approach documents five functional flow components, quantified by 23 functional flow metrics, that describe the key environmental functionality produced historically by California streams (CEFWG 2021; Yarnell et al. 2020) (Figure 1).

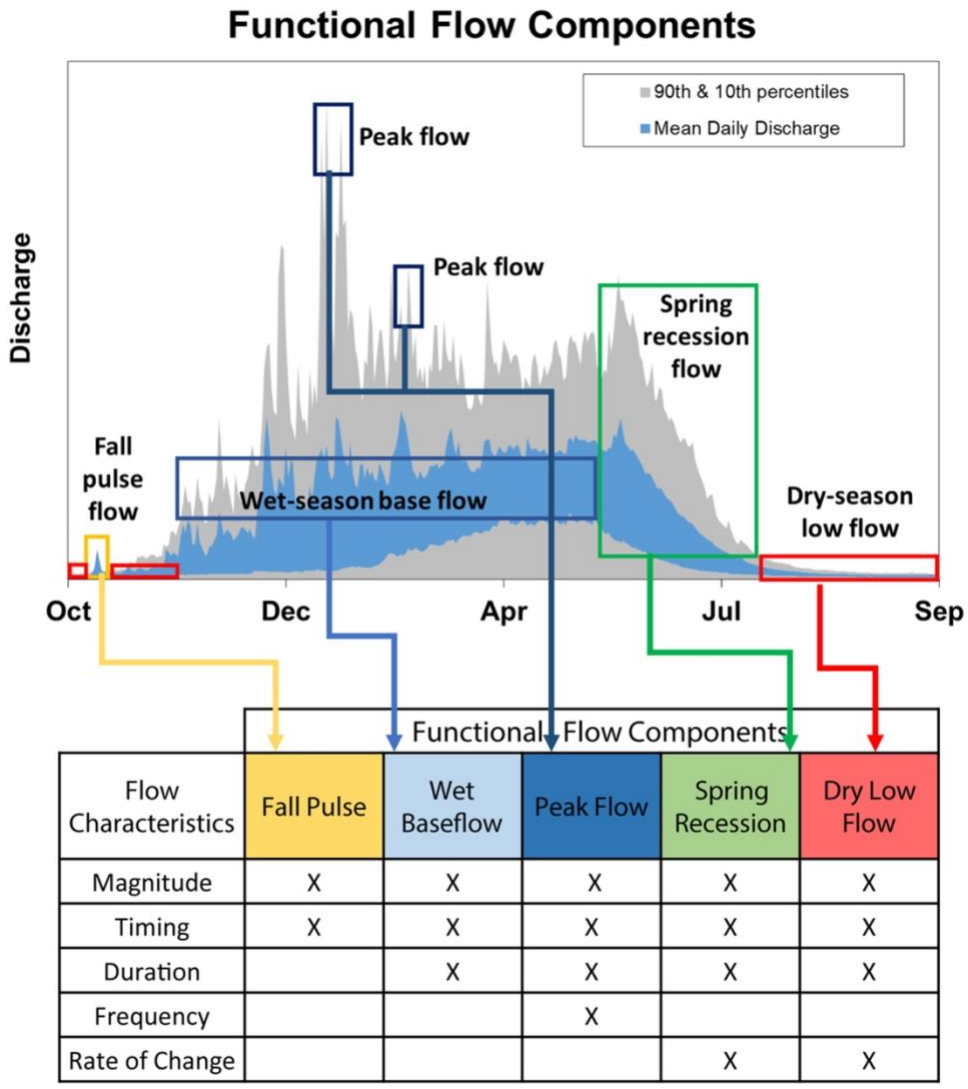

Flow Characteristics	Fall Pulse	Wet Baseflow	Peak Flow	Spring Recession	Dry Low Flow
	Functional Flow Components				
Magnitude	X	X	X	X	X
Timing	X	X	X	X	X
Duration		X	X	X	X
Frequency			X		
Rate of Change				X	X

Figure 1: Five functional flow components (boxes) used to describe the flow regimes typical of California rivers. These five components can be quantified through flow characteristics/metrics shown the table (Yarnell et al. 2020).

Work completed in 2020 by Patterson et al., developed computer code that calculates functional flow metrics in naturalized river systems. This code called the functional flow calculator (FFC) correctly identifies the metrics with 90% accuracy across 223 unimpaired or reference gages in California (Patterson et al. 2020). Since the calculator was built to identify functional flow components in natural systems, it works to smooth the noise in the historical daily flow time

series and identify seasonal and sub-seasonal patterns. This original reference-based calculator will be referred to as the FFC-R for the remainder of this thesis.

However, the FFC-R does not work as well in rivers that have been dammed, diverted, or have flashy flow regimes that do not reflect such predictable seasonality. When the code developed for unaltered river systems was run on flow data from flashy or highly altered streams (i.e. streams below dams or with significant diversions or return flows), the metrics were frequently unable to be identified or were inaccurate. For example, below the rim dams surrounding the Sacramento and San Joaquin Valleys where flows are shifted from the natural wet season to the summer for irrigation and do not have smooth transitions between seasons, the FFC-R was not able to produce accurate metrics for many water years.

Often these anthropogenically altered systems are flat lined for a large portion of the year, with rapid changes from release of irrigation flows or spill events at a dam due to large rainfall events. This flashiness is more similar to small rainfall-dominated systems that alternate between highly variable flows during the wet season and very low stable or intermittent flows in the dry season. These streams are not well classified using the large Gaussian filtering methods developed by Patterson et al (2020) that remove rapid changes characteristic of these streams (Poff et al. 1997). Generally, the more altered or flashy stream systems had worse FFC-R performance.

To accurately measure functional flow metrics from CEFF in naturally flashy streams and highly altered systems, this study produced the Functional Flow Calculator - Flashy (FFC-F). Unlike the FFC-R, the FFC-F minimizes data smoothing and analyzes abrupt changes in flow to identify seasonal changes. The following sections describe the methods used to quantify functional flow metrics in flashy and altered streams (section 2), results on the performance of the FFC-F in

correctly identifying metrics across the water year (section 3.1), a comparison of results from the FFC-F and the FFC-R for a selection of natural flashy streams and highly altered streams (section 3.2), and a process for determining when to use the FFC-R versus the FFC-F to calculate functional flow metrics in a stream (section 4). Section 5 presents two case study applications of the FFC-F on a highly altered stream system and a naturally flashy stream, followed by some brief conclusions in Section 6.

2 METHODS

2.1 Study Area

California's hydrology is complex with diverse geology, climate variability, and extensive water management systems. The state has a Mediterranean climate, with predictable and distinct wet and dry seasons. The Sierra Nevada mountains, particularly its snowpack, provide a critical water supply for ecosystems and people downstream. During the wet season, precipitation is primarily from low-pressure storm cells and atmospheric rivers coming from the Pacific Ocean. This precipitation supports an extensive winter snowpack in the mountains, surface runoff in rivers, and aquifer recharge in the lower valley. The gradual melting of snowpack in the warmer months causes high runoff from mountain watersheds during the spring and early summer. Despite the abundance of water in the winter, most anthropologic uses, such as agriculture, require water during the summer and fall when precipitation is lacking, thus necessitating the large-scale development of reservoirs and water infrastructure.

Water for human needs is gathered, stored, and distributed by dams, diversions, and pipelines across the state. This infrastructure attenuates floods, generates hydropower, and supplies water

in drier areas in normally dry months. Dams significantly modify natural flow regimes, leading to flow regimes that rapidly change between high and low flows and/or stay constant for extended periods. These highly regulated systems deviate greatly from their natural flow regimes associated with nine natural hydrologic regime classes identified for California (Lane et al. 2018).

The flashy ephemeral rain (FER) streamflow class has the lowest mean flow and is the least predictable of the stream classes defined for California (Lane et al. 2018). This class is rain-driven and often has high impervious soil content, resulting in flow regimes with little baseflow and extreme responses to rainfall events. The Function Flow Calculator – Flashy (FFC-F) was designed to accurately calculate metrics for this natural streamflow class, as well as highly altered streams that exhibit similar flashy flow patterns. Because anthropologically affected rivers can also have flow regimes that lack seasonal patterns, are flat-lined, or have unpredictable flows year-round, the FFC-F was also designed to take these irregular patterns into account.

2.2 Study Data

The data for this study came from the United States Geological Survey (USGS), California CDEC stream gages and modeled flow data associated with FERC relicensing and current assessments of dam management.

Two primary types of streams were analyzed:

1. Highly dam-regulated stream systems with flatlined, flashy, or "block hydrographs"
2. Flashy ephemeral rain-driven (FER) streams
    a. These are not altered streams but do not exhibit the same predictable seasonal patterns as the other steam classes.

Both stream types can be characterized as systems with times of rapid rates of change or very little change, i.e., flat-lined flows. Additionally, in the FER systems, there can be large periods of zero flows, which can cause the existing FFC-R to not produce metrics. A list of gages used in the development and testing for this project are presented in Appendix A.

2.3 Alternate Function Flow Identification Algorithm Development

The FFC-F was developed using flow data from primary gages below dams in California often in urban areas, central valley agricultural areas, or the mountain ranges across the state and in the FER streams throughout the state but primarily in coastal ranges and desert areas. The general approach was developed based on the flow rule set described in (Baruch et al. In Review). To mitigate the issues caused by the FFC-R applying smoothing filters, the FFC-F uses very little filtering or smoothing in the calculation process and primarily relies on singular large changes in the flow to indicate seasonal changes. The following sections show in detail how each functional flow component metric is calculated in the FFC-F and how that compares with the original FFC-R. Each component has at least 3 metrics for timing, magnitude, and duration.

2.3.1 Spring Recession

The spring recession is the transition from the wet to dry season and has a steady decline of flows over weeks or longer from snowmelt, shallow subsurface baseflow, and groundwater discharge. The spring recession starts on the last significant peak of the wet season and provides a gradual transition into the dry season. This peak and gradual transition from high-cool flows to low-warm flows triggers cues for migration and reproductive activities and creates varied habitats for a multitude of aquatic organisms (Freeman et al. 2001; Lambeets et al. 2008). This

process also allows for groundwater to be recharged and sediment to settle across the wetted perimeter (Hassan, Egozi, and Parker 2006; Madej 1999; Opperman et al. 2018).

Four metrics describe the spring recession component: timing, magnitude, rate of change, and duration. The FFC-F also includes a fifth metric, the maximum daily rate of change.

2.3.1.1 Timing

The spring recession starts are calculated very differently in the two rule sets. The FFC-R looks for a natural recession using a wide Gaussian filter on the entire water year to find the start of the wet and dry seasons (Patterson et al. 2020). The peak of the filtered hydrograph is identified, and then a window for the spring recession start timing is set as 20 days before the peak until 50 days after (Figure 2). The flow data between these points is then filtered using a much narrower Gaussian filter, and the derivative is found using splines. The FFC-R then goes through the peaks identified in the window from the end backward. The first peak is above the 50th percentile of the filtered data and the slope is above a threshold based on the water year's maximum slope. After the last peak is identified in the narrowly filtered data, then a new window is created from 4 days before that peak until 7 days after. The day with the maximum flow is found in that window. The spring recession start timing is set as the 4th day after the maximum raw data value.

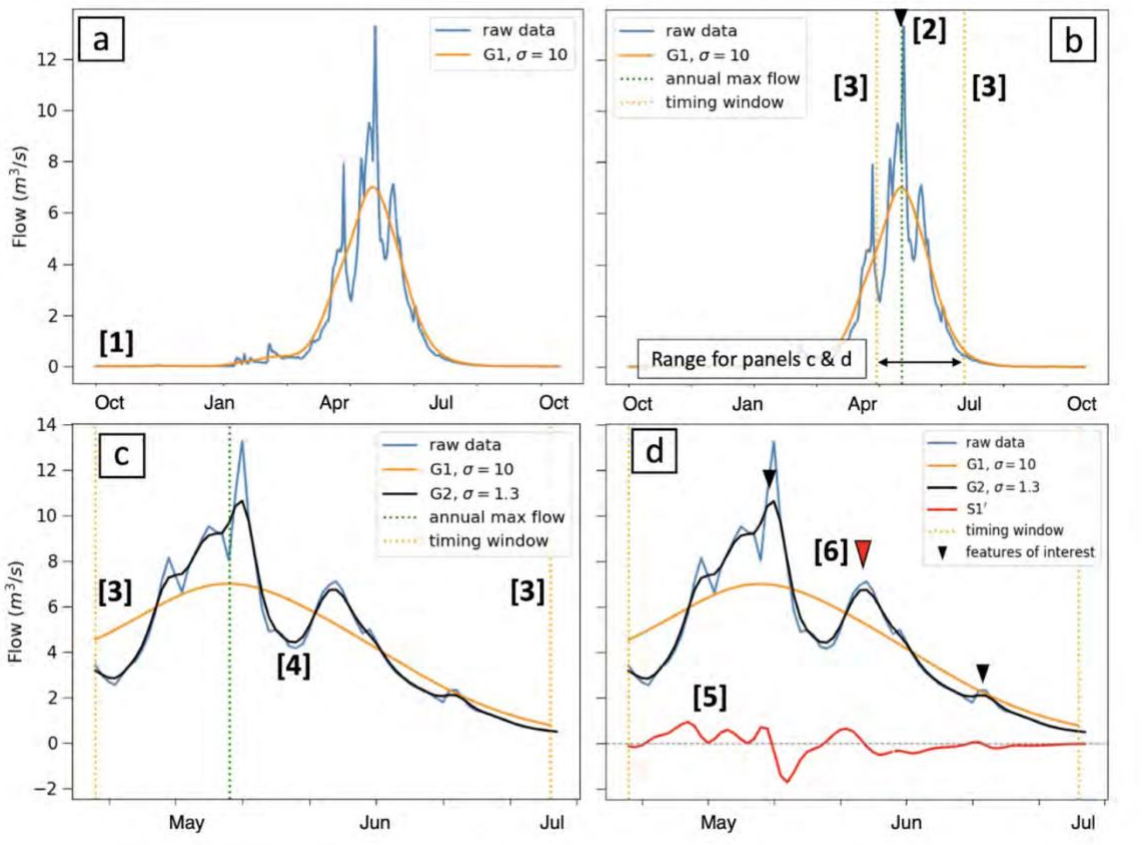

Figure 2: Visualization of Spring Recession Start Timing Identification For FFC-R Rule Set: (a) A wide Gaussian filter is applied to the raw flow data. (b) The global maximum for that water year is found in the filtered data and a timing window is set from 20 days before until 50 days after the global maximum. (c) Within the timing window, a narrow Gaussian Filter is applied. (d) Peaks are identified and the last peak above the 50th percentile of narrowly filtered data that meets the slope threshold is identified as the spring recession start (Appendix C CEFWG 2021).

The FFC-F looks for more abrupt changes in the seasons with a simpler method than the FFC-R. In the FFC-F, there is a narrow Gaussian filter applied to the flow over the entire water year to avoid selecting erroneous peaks on the falling limb of recession as the start of the spring recession. Then the peaks in the filtered data are identified using the findpeaks function from the Pracma R package. The peaks below the 90th percentile flow for that water year and peaks that occur after the 345th day of the water year are removed. The spring peak is then set as the last peak of the water year that meets those criteria. Since a narrow Gaussian filter was applied to the

flow data, the code needs to check that the actual peak is selected. So, the raw flow data from 2 days on either side of the selected peak is analyzed and the day with the maximum flow in that window is selected as the spring recession start timing. A visualization of the process is presented in Figure 3 below.

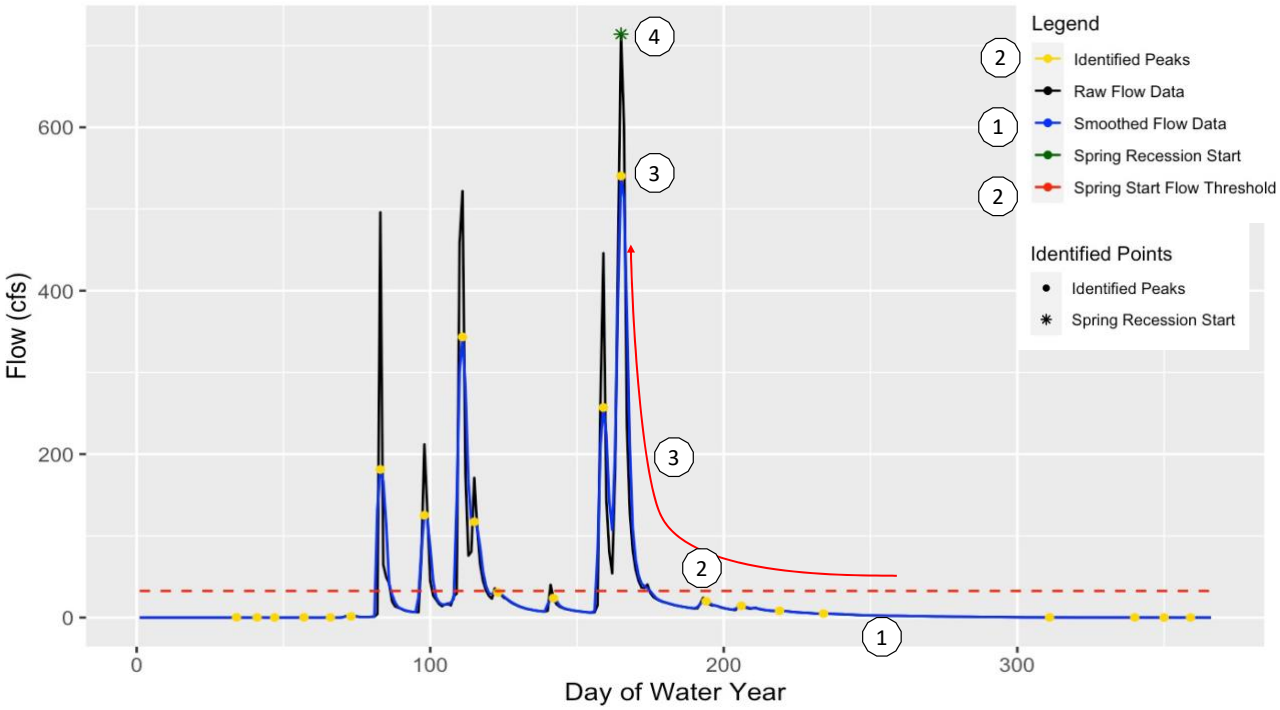

Figure 3: Visualization of Spring Recession Start Timing Identification For FFC-F Rule Set: (1) The Raw flow data for the water year is smoothed using a narrow Gaussian filter. (2) Peaks in the smoothed data are identified. (3) Look backward from the end of the year to find the last peak above the 90th percentile of flow that water year in the smoothed data. (4) The day with maximum flow within 4 days of the peak identified in the smoothed data is selected as the spring recession start date.

2.3.1.2 Magnitude

The magnitude of the spring recession is the flow magnitude on the date of the spring recession start. The magnitude is calculated the same for both FFC-R and FFC-F.

2.3.1.3 Rate of Change

The rate of change in both calculators is defined as the median rate of change value for all negative (decreasing flow) rate of change values between the spring recession start timing and the dry season start timing.

2.3.1.4 Maximum Rate of Change

FFC-F has an additional metric called “Maximum Rate of Change”. This metric reports the largest single daily negative rate of change value during the spring recession. This metric was added to the FFC-F, since flashy systems river systems can frequently have a short period of large change followed by little to no change in flow. In these cases, the “Rate of Change” metric can be misleading. Hypothetically if there are 3 days with large flow changes (25%) and there are 4 days with little flow change (3%) then the “Rate of Change” metric will report 3% as the median value, which is not accurately describing the rate of change that system experienced. The maximum rate of change reports the value from periods of extreme change during the recession, while the original rate of change metric could identify a value from a period of relatively mild rate of change. The maximum rate of change metric is important in understanding whether native species like cottonwood, which require small stage changes during periods that often align with spring recessions, are being properly managed for (Lytle and Merritt 2004; Shafroth et al. 1998).

2.3.1.5 Duration

The spring recession duration for both the FFC-R and FFC-F is calculated as the number of days from the start of the spring recession until the dry season start timing.

2.3.2 Dry Season

The dry season baseflow is sustained by groundwater during a long period when rain is usually absent in the summer months. These flows are generally low and may involve the stream going dry, and they typically have lower within-season and interannual variability than other flow

components. The low dry season flows provide an important ecological function allowing native Californian species that have adapted to these low flows to survive and preventing non-native species from gaining a foothold in the ecosystem (Baruch et al. In Review). If these flows are similar to predevelopment low flows, they can help limit non-native species from establishing (Lee and Suen 2012; Postel and Richter 2015; Yarnell et al. 2015).

The dry season is represented by four metrics: the timing, the median baseflow magnitude, the 90th percentile high baseflow, and the duration.

2.3.2.1 Timing

In the original FFC-R, the dry season start timing is found by applying a wide Gaussian filter to the entire water year. Once the data is filtered, then the filtered data has splines fitted to it and the slope is calculated. The major peaks in the filtered data are identified and the last peak of the water year is selected as the starting point to look forward to find the start of the dry season. The splines and their slope after the last peak are used to find where both fall below a threshold. The day when this occurs is set as the start date of the dry season.

The rule set for FFC-F also looks for the flow to drop below a certain rate of change and flow thresholds to trigger the start of the dry season. The main difference is that the FFC-F does not use a Gaussian filter and it uses the spring timing for where it starts to look for the dry season start instead of analyzing the entire water year. The exact rule set for the FFC-F is either to look for the first consecutive five days that has a daily rate of change less than 2%, or if the flow is below 50 cfs, look for the first consecutive five days that flow changes by 2 cfs or less. There is also a minimum flow threshold that these consecutive days must be below, which is the same as

the flow threshold set in the FFC-R and is defined in equation 1. If more than half of the days had increasing or unchanged flow, then the first day of the five consecutive days is selected as the start of the dry season, otherwise, the dry season start timing is set as the last day of the five consecutive days.

$$DS_{thresh} = Q_{min_{postSP}} + (Q_{max_{WY}} - Q_{min_{postSP}}) * P_{DS_{Start}} \quad (1)$$

Where:

DS_{thresh}, is the threshold for the dry season to start;

$Q_{min_{postSP}}$, is the minimum flow after the spring recession start timing;

$Q_{max_{WY}}$, is the maximum daily flow during the entire water year;

$P_{DS_{Start}}$, is a percent that sets how much larger than the minimum flow the threshold is.

In the FFC-F, the $P_{DS_{Start}}$ parameter used in the equation was set to 0.125, which is similar to the FFC-R calculator.

In water years where a dry season start is not identified from the above rules, then the rate of change threshold is changed to 5% and the analysis is conducted again. If again a dry season timing is not found, then the consecutive day threshold is decreased to 3 days. A visualization of the entire FFC-F process is presented in Figure 4 below.

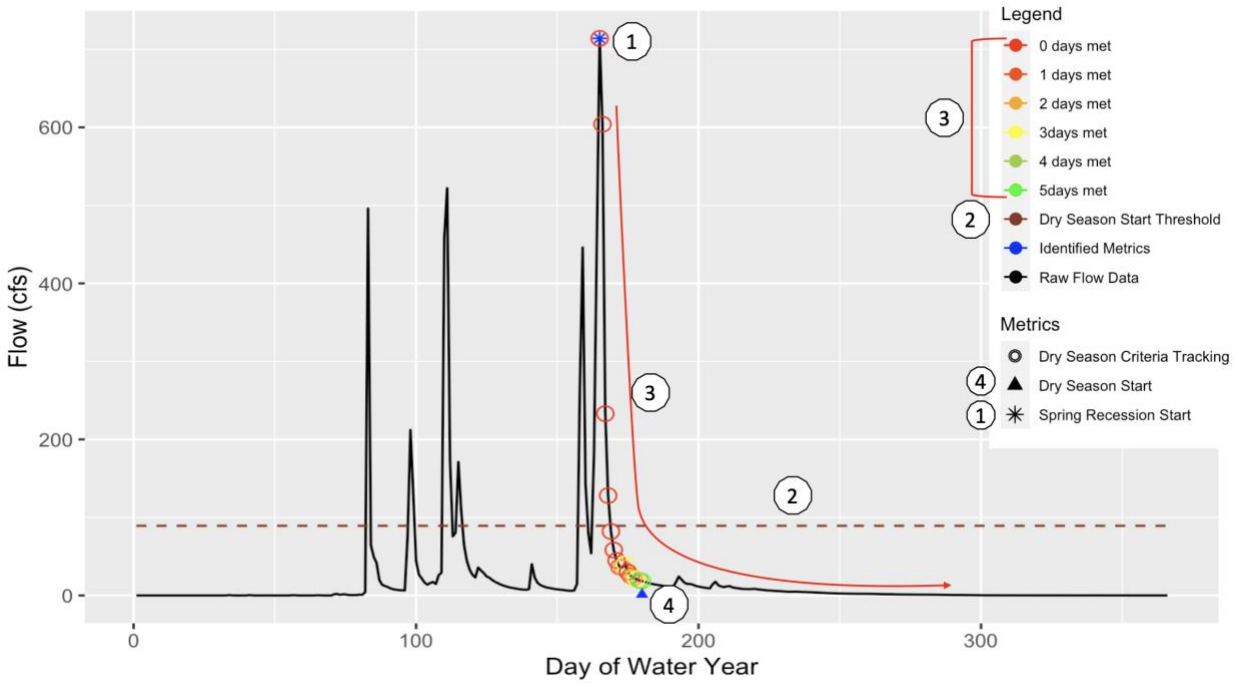

Figure 4: Visualization of Dry Season Start Timing Identification For FFC-F Rule Set: (1) The raw flow data and previously calculated spring recession are loaded in. (2) The dry season start threshold is set using Equation 1. (3) Going forward from the start of the spring recession each day is tested to see if it meets the dry season start criteria. (4) Once there are five consecutive days meeting the dry season start criteria then the dry season start is selected.

2.3.2.2 Magnitude

The dry season has two magnitude metrics. The first is median baseflow, which is the 50th percentile of daily flows from the start of the dry season until the start of the wet season. This value is reported as the baseflow for the dry season. There is also the dry season high-baseflow, which is the 90th percentile of daily flows from the start of the dry season until the start of the wet season. These magnitude metrics are calculated the same way in both the FFC-R and FFC-F.

2.3.2.3 Duration

The duration of the dry season is the number of days from the dry season start timing until the start of the wet season. This metric is calculated the same way in both the FFC-R and FFC-F.

2.3.3 Fall Pulse

The fall pulse results from the first major storm at the end of the dry season. This event signals the coming of the wet season for the river ecosystem. The fall pulse provides ecological benefits to native Californian species such as fish migration and flushing fine sediment/organics (Yarnell et al. 2015).

Three metrics are produced to represent the fall pulse component by both calculators, including the fall pulse timing, magnitude, and duration. The FFC-F also produces a new metric, Fall Difference, quantifying the difference between the fall peak magnitude and the previous dry season baseflow. This metric provides a continuous measure of how large a fall pulse is relative to the dry season baseflow, where a value of zero implies a pulse did not occur during the fall timing window.

2.3.3.1 Timing

To find a fall pulse in the FFC-R, a narrow Gaussian filter is first applied to the flow data for the water year. Then the filtered data is analyzed for peaks. For a fall pulse to occur, one of the peaks must be at least 1.5 or two times the dry season baseflow depending on the magnitude of the precious water year's dry season baseflow. If there are only pulse flows less than this threshold or if a peak occurs before October 1st or after December 15th, then the fall pulse component is said not to have occurred and the calculator returns an N/A.

In the FFC-F, the process is like the FFC-R; however, the FFC-F does not use a Gaussian filter and the threshold is set to 1.5 times the previous water year's dry season baseflow. Otherwise, the rule set is very consistent with the original FFC, with the pulse needing to occur between

October 1st and December 15th. Once a qualifying pulse is found, the timing is set at the maximum discharge of the peak, or if the qualifying peak has a plateau, the timing is set as the first day of the plateau. These rules can be visualized in Figure 5.

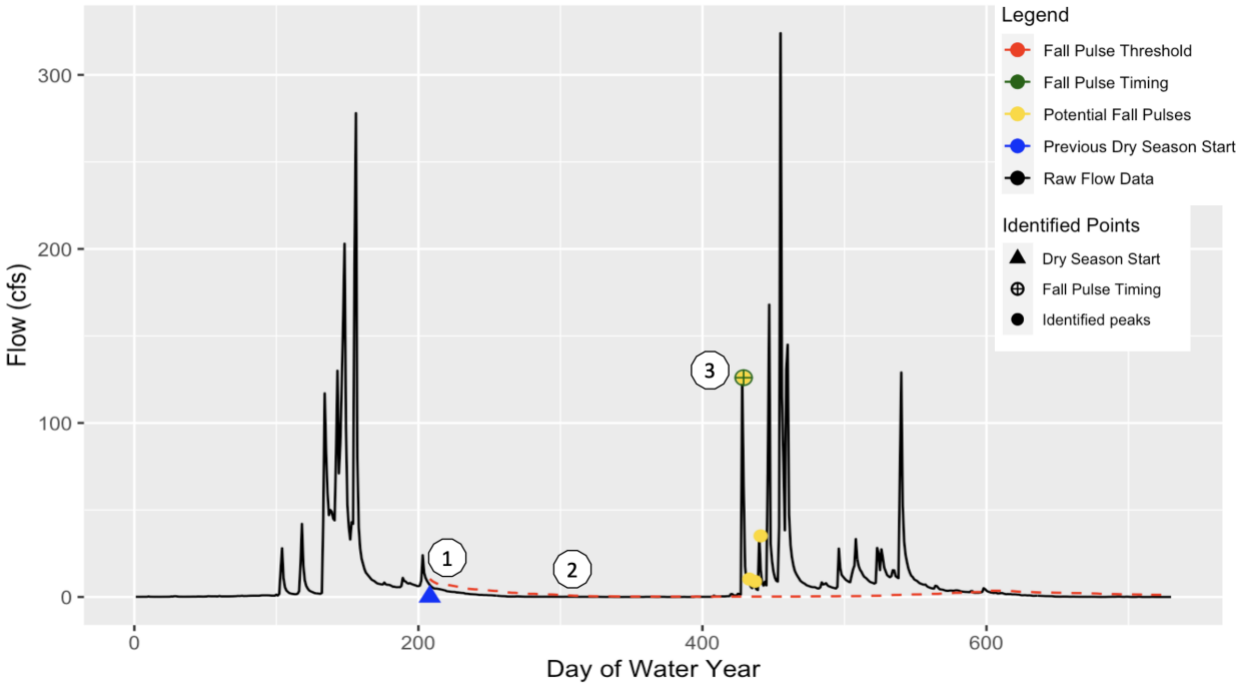

Figure 5: Visualization Fall Pulse Timing Identification For FFC-F Rule Set: (1) The previous dry season start timing and raw flow data for the previous and current water year is loaded. (2) The flow data after the previous dry season start has a running median taken, which is then multiplied by 1.5 for the threshold for the fall pulse to occur. (3) Peaks are identified between October 1st and December 15th of the current water year. The first peak above the threshold is selected as the fall pulse for the current water year.

2.3.3.2 Magnitude

The magnitude of the fall pulse is the flow value at the day of the timing. This metric is measured in day of the water year for both the FFC-R and FFC-F.

2.3.3.3 Duration

The CEFF guidance document defines the duration of the Fall pulse as the number of days from the start of the rising limb until the end of the falling limb of the Fall pulse peak (CEFWG 2021). The FFC-R defines the duration of the fall pulse as the start of the rising limb until the fall pulse timing at the fall peak magnitude. To allow for proper comparisons between the two calculators, the fall pulse duration in the FFC-F was given the same definition as the FFC-R.

2.3.3.4 Fall Difference

The fall difference is a new metric in the FFC-F. This metric reports the difference between the fall pulse peak magnitude (or if there wasn't a fall pulse identified, the largest flow peak in the fall timing window of October 1 to December 15) and the previous water year's dry season 50th percentile baseflow. If this metric is equal to or greater than half the last dry season 50th percentile baseflow, then a fall pulse should be reported. If flow is flatlined through the fall season (no peak or pulse event occurred), then this metric value would be zero. It is possible in rare occasions that this metric can be negative if flows are decreasing or if flows are higher early in the dry season, such that peak flows in the fall pulse timing window are lower than the 50th percentile base flow. This metric is measured in cfs, similar to the magnitude metrics.

2.3.4 Wet Season Baseflow

A wet season should occur each water year when flows are generally higher than the rest of the year. In California, this generally aligns with the winter and early spring months. These flows provide connectivity throughout the river system allowing for fish migration and replenishing groundwater in the riparian areas (Yarnell et al. 2020).

Four metrics constitute the wet season baseflow component: wet season start timing, the 10th percentile baseflow magnitude, the median baseflow, and duration.

2.3.4.1 Timing

The FFC-R initially smooths the raw flow data using a large Gaussian filter to identify the water year's global peak and preceding global valley. A relative magnitude threshold is then established based on the difference between the peak and valley, with a scaling factor so the wet season is identified before significant increases in flow. Subsequently, a spline curve is fit to the smoothed data so that the slope of the data can be easily evaluated. Finally, starting at the global peak and looking backward in time until the flow is below the set threshold and a slope is below a threshold set based on the global peak, the first day that meets both thresholds is set as the start of the wet season.

There are three main differences between how the wet season start timing is calculated in the FFC-F: no data smoothing, forward-looking, and there is no rate of change threshold. Since the dry season does not end until the wet season begins, the wet season threshold is found by computing a rolling median of flow from the previous water year's dry season start timing through the end of the current water year, which is then multiplied by 1.5 to set a rolling threshold to identify the start of the wet season (Figure 6). The start of the wet season is calculated by finding the first date where flow is greater than the rolling threshold after the fall pulse. If there was no fall pulse, then the wet season start timing is the first day after the fall pulse window that is greater than the rolling threshold.

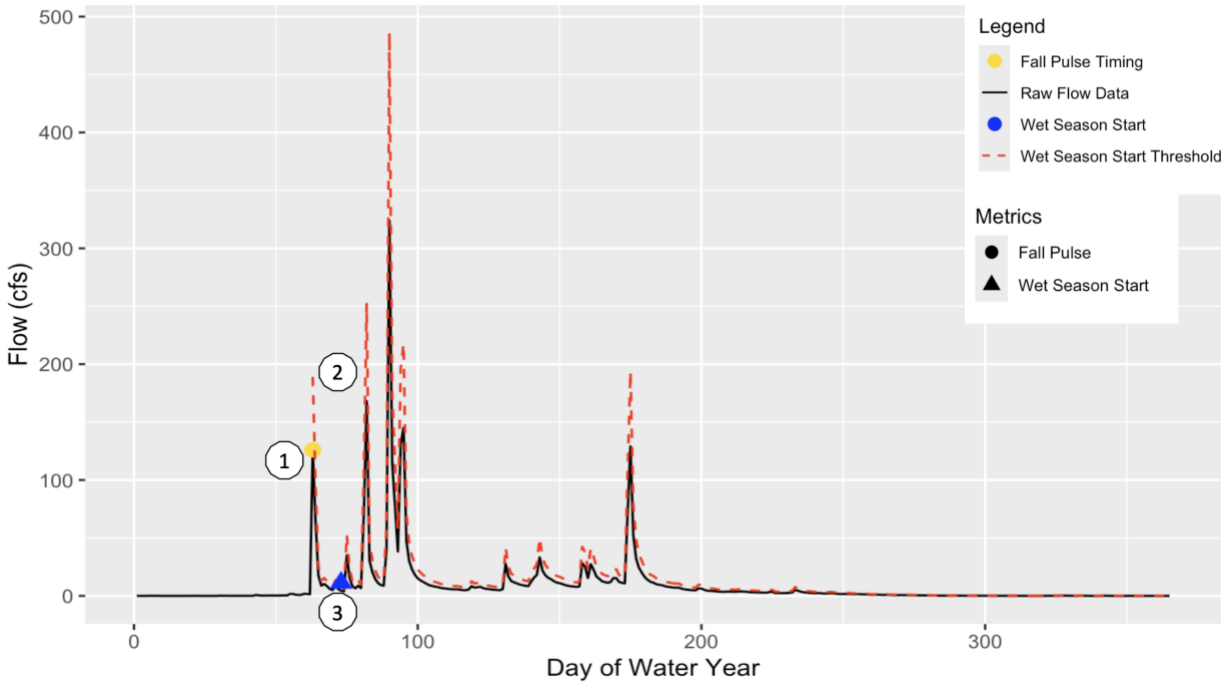

Figure 6: Visualization Wet Season Timing Identification For FFC-F Rule Set: (1) The raw flow data and the fall pulse are loaded in. (2) The rolling median of the flow data after the fall pulse is compared to that same value multiplied by one and a half to set the threshold for the wet season starting. (3) the wet season is selected as the first day above the threshold.

2.3.4.2 Magnitude

There are two magnitude metrics associated with the wet season. The first is the wet season baseflow, which is the 10th percentile of daily flows from the start of the wet season until the start of the spring recession. The second is the wet season high-baseflow, which is the 50th percentile of daily flows from the start of the wet season until the start of the spring recession.

These magnitude metrics are calculated the same way in both the FFC-R and FFC-F.

2.3.4.3 Duration

The duration of the wet season is the number of days from the wet season start timing until the start of the spring recession. This metric is calculated the same way in both the FFC-R and FFC-F.

2.3.5 Peak Flow Prediction

The wet season peak flows are produced by the largest storm events in the wet season. These flows help reform and shape the river channel and banks by scouring the river and transporting sediment and woody debris (Yarnell et al. 2020). These high flows and associated scour will disrupt the establishment of non-native species allowing for more diversity in the riparian flora and greater habitat diversity over time (Yarnell et al. 2015). They also help reform and shape the river channel and banks by scouring and transporting sediment and woody debris (Ward 1998) and disrupt the establishment of non-native species, allowing for more diversity in the native riparian flora (Petts and Gurnell 2013).

Four metrics represent the peak flows for each of the three flood-frequency return intervals.

2.3.5.1 Magnitude

The 2-, 5-, and 10-year flood flow magnitudes are calculated by finding the maximum daily flow for each water year. The 50th, 20^{th,} and 10th percentile of these peak flows are then calculated to approximate the 2-, 5-, and 10-year flood flows respectively. While it is standard of practice to fit peak flow to a Log-Pearson Type III or a Gumbel distribution, the default for the FFC-F is to calculate the peak wet season flows using the same statistical approximation method as the FFC-R so that the results could be directly compared. Once these flood flow values are calculated, each water year is checked to see if qualified flow events cross the flood flow threshold.

This statistical method of approximating flood flows is limited by available data. For a gauge with 15 years of flow data, there is only about an 80% chance that the site has experienced a 10-year flow event. If that gauge with a 15-year record never records a flow that is equal to or larger than the actual 10-year flood event (from a hypothetical 100-year period of record), then the calculator will produce inaccurate results for the estimated 10-year flood event. To mitigate the chances of this happening, the FFC-F can instead use a Log-Pearson Type III distribution to calculate the flood exceedance values, which is a flood frequency calculation method recommended by the United States Geological Survey ("Bulletin_15_1967.Pdf," n.d.).

The Log-Pearson Type III (LPIII) analysis that can be completed in the FFC-F uses exclusively site/station skew. Only using station skew subjects the LPIII analysis to be greatly affected by extreme events shifting the skew in the analysis (USGS 1982). To mitigate this, a general or regional skew is frequently used in analysis in conjunction with the station skew. The generalized skew is found by calculating the skew for gages in a region and then developing an isohyetal map or some aerial relationship that can be used to minimize the station skew that can affect the flood frequency calculations.

Once the magnitude thresholds of the 2-, 5-, and 10-year flood flows are calculated, they are reported as the flood exceedance magnitudes in every year of output. However, the peak magnitude of flow events that meet or exceed the flood thresholds in any given year is not reported.

2.3.5.2 Duration

The duration metric is the sum of all days in qualified events for each of the 2-, 5-, and 10-year flood flows in a particular water year. The peak flow duration in the CEFF Guidance document is defined as the median number of days that a flow event stays over the peak flow magnitude threshold for each of the 2-,5-, and 10-year peak flow events. However, the FFC-R calculates the duration as the total number of days that exceeds the magnitude threshold in a given water year. To allow for proper comparisons between the two calculators, the peak flow duration in the FFC-F was given the same definition as the FFC-R.

2.3.5.3 Frequency

Each event that exceeds each flood threshold is counted towards the frequency metric for that water year. The peak flow frequency is the number of times that the flow crosses the magnitude thresholds calculated for the 2-,5-, and 10-year peak flow events in a water year. This definition is the same for both the FFC-R and FFC-F.

2.3.5.4 Timing

The timing of the peak flow metric is the median timing of the flow events that the magnitude threshold is crossed during a single water year. This is calculated for the 2-,5-, and 10-year peak flow events. This definition is the same for both the FFC-R and FFC-F.

3 Results

The ruleset outlined in Section 2.3 was developed and coded using R version 4.4.0 "Puppy Cup" in RStudio. The current version of the code is available for download from GitHub at the following location: https://github.com/camcarpenter6/Alternate-Ruleset-FFC-BETA. The code

and rule set were developed using the "Functional Flow Calculator – Flashy Development Gages" identified in Appendix A.

The R code package will calculate functional flow metrics using the FFC-F ruleset, visualize the metrics on plotted daily flow data, and compare the FFC-F metrics to the FFC-R metrics.

3.1 Functional Flow Calculator – Flashy Performance

The FFC-F rule set and code were developed to help accurately characterize flashy stream systems using the California Environmental Flows Framework (CEFF) and it does an excellent job at identifying the metrics (Table 1). However, the FFC-F code does not perfectly predict the functional flow metrics in all years and some errors exist that could be examined in future research.

To understand potential errors in the FFC-F, a visual assessment of metrics calculated at the gages used for the development of the FFC-F was completed. This visual assessment involved examining the flow data and metrics for each water year of each gage listed in Appendix A looking to see if the metrics generally align with the definitions of the metrics described in CEFF. Some of the errors observed through the performance analysis included early identification of the wet and dry start season timing prior to baseflows actually changing and late identification of the spring recession start timing after the dry has already started. Table 1 lists the currently identified issues, the stream types they are found in, how they were determined to have happened, and the frequency they occurred. Developing or further analyzing the rules presented in this document may help reduce the frequency of these errors.

Table 1: Issues in Timing Observed in the FFC-F For Flashy Ephemeral Streams and Highly Altered Streams

Metric Timing Issue	Stream Types	Issue	Assessment Criteria	Frequency of Issue in Development Gages
Fall – October 1st	All	In some cases, the fall pulse timing (peak of the pulse) occurs on October 1st. In these cases, there is no rising limb for the algorithm to identify a pulse as a pulse and thus it will be erroneously missed.	Was there a qualified peak on first day of the water year (October 1st)	1%
Early Wet Season Start with Fall Pulse	All, but generally in more naturalized systems or low flow systems	Occasionally there is a fall pulse that occurs then flow returns to the dry season baseflow. After the flow returns to the dry season baseflow, causing the median flows after the fall pulse to approach dry season median baseflow, there is another early season storm causing a spike in flow that then returns to the baseflow. This triggers the FFC-F to identify the start of the wet season even though baseflows are not increasing.	A wet season start is identified on an early season storm event before base flows have started to increase.	2%
Early Wet Season Start without Fall Pulse	Low flow systems	This usually occurs in low flow systems where dry season baseflows near zero. Having such a low dry season baseflow means that practically any increase in flow will trigger the FFC-F to start the wet season, even if it is not a good indicator of the wet season starting, such as a consistent increase in baseflows or a substantial flow event.	A wet season start is identified before there is an increase in baseflows, or a flow occurs.	4%
Late Spring Recession Start	Low flow systems	This usually occurs in systems with dry season baseflows near zero. These systems are also frequently intermittent, and often have a 90th percentile flow for a water year of 0 or near 0. So, if an early rain fall event in early September of August, then it will be identified as the spring pulse and recession.	Spring recession starts in August or September after a long period of low flow beforehand (>1 month) since other flow events.	1%
Early Dry Season Start Identification	All, mostly in natural systems or stepped recessions (dam regulated systems)	On the spring recession after the spring flow threshold is met, if there is a period of relatively flat flows (rate of change less than 2%-5%) then the FFC-F will identify the start of the dry season even if there was still a substantial ramp down period after the flatlined period.	Dry season is identified with a substantial ramp down still needing to occur on spring recession.	4%
Late Dry Season Start Identification	All, but typically in higher flow volume systems.	While trying to find 5 consecutive days at or below the rate of change threshold, flows vary enough day to day to consistently stay above the required rate of change until after the dry season should have been identified.	Dry season identified after a relatively steady baseflow as already been reached.	3%
No Dry Season Start Identified	Typically in inverted hydrographs (wet season in summer months)	The spring recession start timing is correctly identified late in the water year (typically in August or September). However, there is not enough time for the code to then find a start to the dry season prior the water year ending.	No dry season start identified by the code	2%

From Table 1, it is apparent that the FFC-F does an excellent job of accurately identifying metrics. The calculator was accurate in identifying timing metrics in about 95% of the water years analyzed from the development gages (Appendix A). The issue that was most frequent was the early identification of the wet season, occurring both with and without a fall pulse in 6% of the water years. The next most frequent issue was the early identification of the dry season start, which occurred 4% of the time. This was more frequent in some altered systems where flow schedules as designed with stepped recessions, which can allow the flow to go just below the magnitude threshold, and then flatline for a week. This triggers the dry season start timing identification even if further step downs are planned. In this error analysis, it is important to disclose that because it is a visual analysis, there is some level of subjectivity by this author. Additionally, the analysis was conducted on the gages used to design the ruleset, and if analyses were conducted on other gages or by another individual, the frequency of the errors occurring would likely change.

3.2 Functional Flow Calculator Comparison

Since the FFC-F was developed for flashy systems, it is important to understand how its results compare to the FFC-R, which is currently used as the functional flow metric calculator for all systems. To better understand the differences in the calculators, the results of each calculator for the gages that the FFC-F was developed for were compared. The gages included the reference gages for Class 7 (Flashy Ephemeral Rain Driven Streams) and a set of gages for several highly altered streams that selected by the author and project collaborators.

A comparison of timing metrics produced by the two calculators for the sets of gages are presented in Table 2. The reason timing metrics are the only metrics compared is that other metrics (except wet season peak flow metrics) are directly tied to the timing metrics.

Table 2: Difference between timing metrics for the FFC-R and FFC-F in two sets of gages (FER and highly altered streams) using criteria based on the number of days of difference in timing

Stream Class Category	Metric	Percent of Metrics Meeting Criteria			
		|(FFC-F) -(FFC-R)|<= 3 days	3 days <|(FFC-F) -(FFC-R)|<=7 days	7 days < |(FFC-F) -(FFC-R)|<=14 days	14 days <|(FFC-F) -(FFC-R)|<=30 days
Flashy Ephemeral Rain (FER)	Fall Timing	59.3	5.3	5.3	13.3
	Wet Season Timing	8.5	16.7	19	27.5
	Spring Timing	41.4	24.5	3.9	11.9
	Dry Season Timing	1.8	3.2	8.4	24.4
Highly Altered Systems	Fall Timing	63.4	7.6	5.9	12.6
	Wet Season Timing	12.5	9.4	12.3	20.7
	Spring Timing	43	11.5	9.7	15
	Dry Season Timing	6.8	9.6	12.9	24.1

Stream Class Category	Metric	Percent of Metrics Meeting Criteria			
		30 days <|(FFC-F) -(FFC-R)|<=60 days	60 days < |(FFC-F)-(FFC-R) |	(FFC-F) -(FFC-R) > 3 days	(FFC-F) -(FFC-R) < (-3) days
Flashy Ephemeral Rain (FER)	Fall Timing	15	1.8	39.8	0.9
	Wet Season Timing	20	8.3	49	42.6
	Spring Timing	11.7	6.6	13.4	45.3
	Dry Season Timing	30.1	32.1	4	94.2
Highly Altered Systems	Fall Timing	9.2	1.3	30.3	6.3
	Wet Season Timing	20.1	25	40.4	47.1
	Spring Timing	10.6	10.3	36	21
	Dry Season Timing	21.2	25.3	8.4	84.8

Across both sets of gages, there are a few notable trends in timing metrics. In the two groups, the fall pulse timing and the spring recession start timing align closely between the two calculators, with ~60^{+} % of Fall Pulse Timings being within 3 days of each other and 40^{+} % of the spring recession start timings being within 3 days of each other.

The timing metric that are the most divergent between the two calculators is the dry season start timing, where more than 14 days difference occurs in more than 70% of years (Table 2). Additionally, the dry season start timings produced by the FFC-F are at least 3 days earlier than the metrics produced by the FFC-R in ~85^{+}% of water years in both sets of gages. These two trends imply that the FFC-F consistently produces dry season timings that are earlier than the FFC-R. This trend has carry-over effects on the rest of the dry season metrics and the spring duration and rate of change metric.

A similar trend occurs with the wet season start timing between the two calculators with 55^{+} % of the water years having timings at least 14 days apart. This is very similar to the dry season trend; however, it differs in that there is not a clear trend in whether the wet season start timings produced by the FFC-F are earlier or later than the FFC-R, as both 40^{+}% of water years had timing occurring 3 days or more earlier and 40+% of water years had timing occurring 3 days or more later.

3.2.1 Flashy Ephemeral Rain-Driven Systems

Flashy Ephemeral Rain-Driven (FER) streams are the only natural systems in which the FFC-F was designed to accurately predict metrics. These systems have similar trends as the other rain-

driven systems but are generally more pronounced. This stream class is characterized by the lowest mean annual flow and the longest periods of extremely low flows. This system also has the lowest predictability (Lane et al. 2018). These trends make FER streams the only natural stream class that has similarities to the highly altered systems discussed in the subsequent section.

The lack of predictability is apparent with the fall pulse, where FER streams have the least number of matching metrics between the calculators at approximately 60% (Table 2). Additionally, FER streams have the most fall pulse timings that differ between the calculators by over 14 days, at about 30% of water years. Of the 40% of metrics that don't match, over 95% of the fall pulse timings produced by the FFC-F are later than the metrics produced by the FFC-R.

As mentioned in the previous section there is a large difference in the wet season start timing produced by two calculators. The substantial difference in wet season timings can be best explained by the difference in the calculation method. FFC-R uses a back-stepping calculation based on thresholds computed based on the maximum flow of highly smoothed data for the water year in being calculated. FFC-F, however, uses a forward-stepping calculation with thresholds based on either the preceding dry season baseflow or the time between a fall pulse and the wet season start. As seen in Figure 7, the FFC-F does much better at predicting the wet season start timing in a reference gauge for the example FER system.

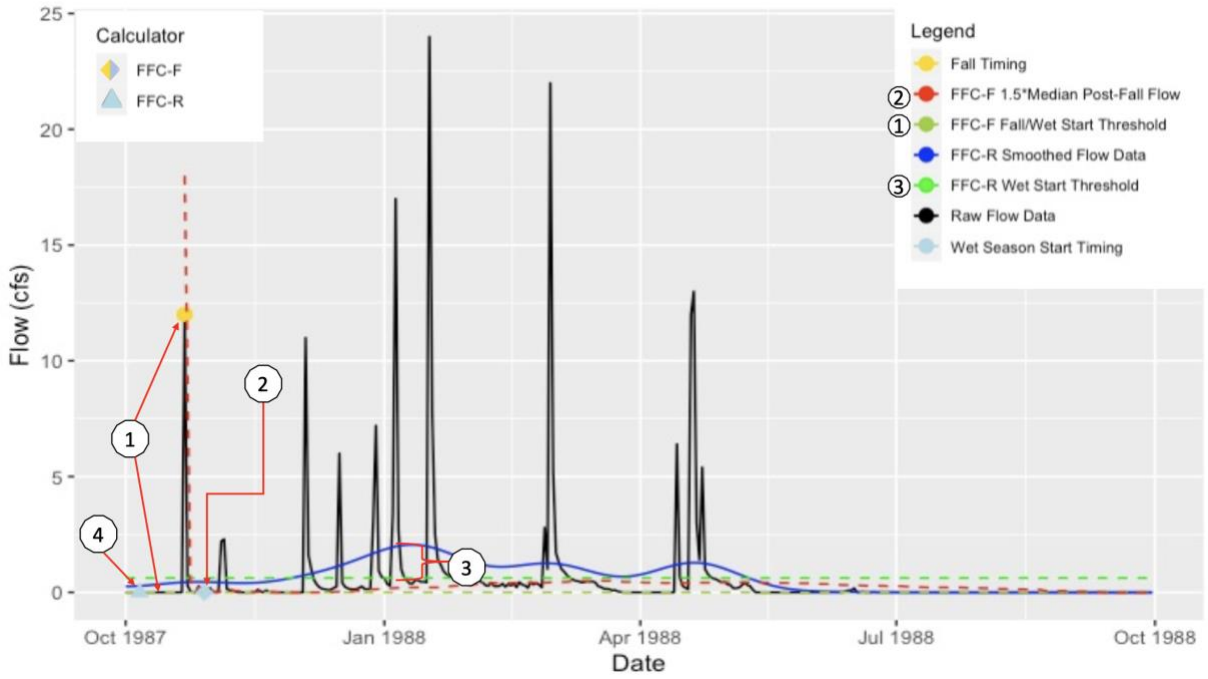

Figure 7: In a reference FER stream (USGS gage ID: 11120510, San Jose Creak at Goleta, CA) in Water Year 1988. (1) A fall pulse is detected by FFC-F when a storm event causes a return flow over the fall threshold (olive dashed line). (2) FFC-F then looks forward until there is a day with flow equal or greater than one and a half times the running median of flow after the fall pulse. (3) FFC-R uses the smoothed data to set a flow and slope threshold. (4) FFC-R then looks backwards until both are met in this case the slope threshold (not shown) is not met until near the beginning of the water year. The wet season timing is so early that FFC-R does not count the fall pulse that occurs. In this case FFC-F more accurately predicts the wet season start and identifies an accurate fall pulse that FFC-R does not.

Figure 7 shows USGS Gage ID 11120510 in WY 1988. Due to the wide Gaussian filter used in the FFC-R, there is a substantial decrease in the large peaks that occur during the wet season. This greatly lowers both the thresholds that the filtered flow and its derivative need to go below for the wet season to start. This then leads to the timing for the start of the wet season being pushed approximately two weeks before there is any change in the actual flow. Whereas the FFC-F does not use smoothing and the threshold for the wet season to start is based on the previous dry season. So, timing for the start of the wet season is not triggered until the first

substantial peak of the year. From a visual analysis, the timing produced by FFC-F in this instance is much more accurate.

Similarly comparing dry season timing metrics, the FER streams have the lowest number of timings that match within 3 days of each other, only ~2%, and the highest percentage of timings over 14 days apart at ~87% (Table 2). Of the timings 3 days or more different, 95% of the metrics produced by the FFC-F are earlier than the timings produced by the FFC-R.

One of the major reasons that the dry season start timings are so different between calculators and is much later in the FFC-R, is how the flow threshold is calculated. Both calculators use Equation 1 to calculate the flow threshold. However, the FFC-R uses the equation on broadly filtered data, which substantially decreases the maximum flow value used to calculate the threshold and leads to a lower flow threshold that needs to be crossed for the dry season to be identified. In the FFC-F, the same equation is used on the unfiltered data leading to a higher threshold and a generally earlier dry season start. The smoothing in the FFC-R decreases the flow threshold and decreases the slope threshold required for the dry season start to be selected. Whereas the FFC-F has set specific slope thresholds regardless of the range of flows observed.

Finally, the FFC-R finds the dry season start using a broad filter. This will push the start of dry season timing further out (later) than in unfiltered data. This is especially notable in flashier systems where a spring recession can occur over just a few days. If a broad filter is applied to a short flashy spring recession, it will extend the spring recession well past when it ended.

A great example of this is from water year 1960 at USGS gage 11138500 (Sisquoc River Near Sisquoc, CA) (Figure 8). This is a reference gage for FER gages, where both calculators found the same spring recession start timing on April 29 (the FFC-R is 4 days after FFC-F spring recession start timing due to the 4-day lag in the FFC-R). The FFC-F chose a dry season start timing on May 4th when flows start to flatline. However, the FFC-R chose a dry season start timing on June 27th after two months where the flow changed a total of less than ten cfs.

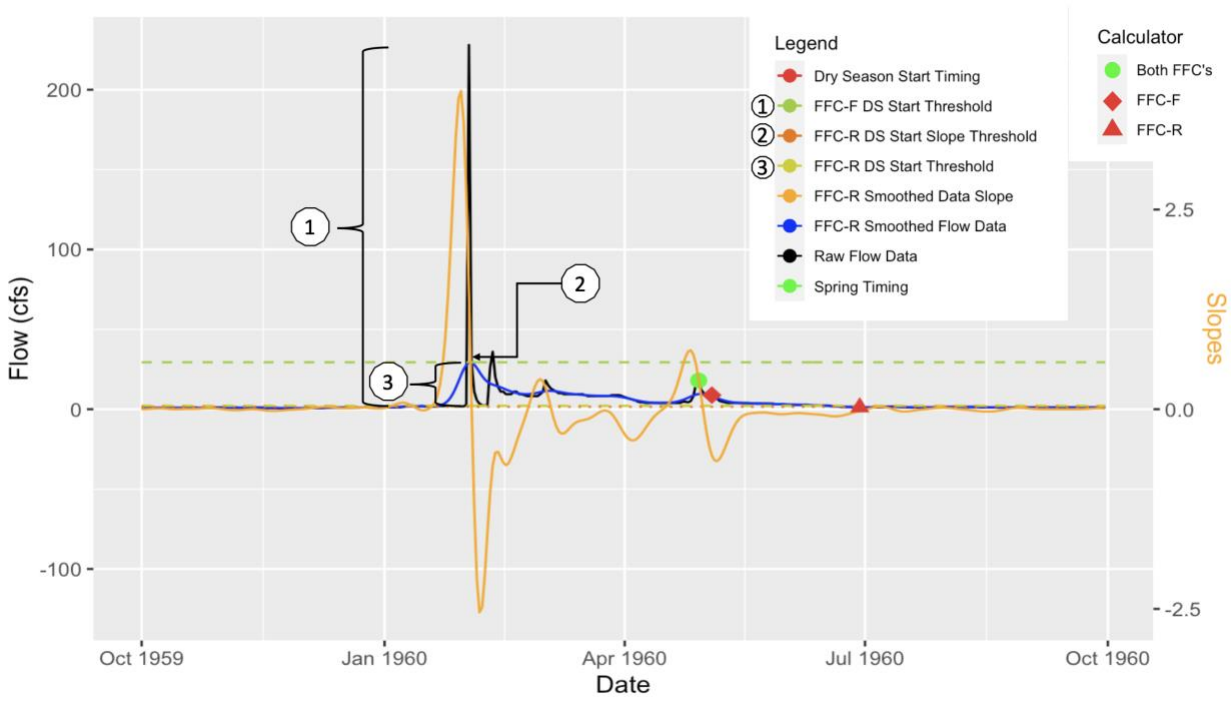

Figure 8: Calculator Dry season start comparison at USGS gage 11138500 (Sisquoc River Near Sisquoc, CA), and FER reference gage, during water year 1960. (1) One large peak during the wet season set a higher dry season start threshold [light green line]. (2/3) The smoothed data reduces peak in the wet season by approximately an order of magnitude (~250 cfs to ~25 cfs), which in turn sets a low flow threshold and slope threshold in FFC-R. This low threshold means

that it takes a long time for both flow data to satisfy both thresholds even though flow had been practically flatlined for months.

These differences in calculation methods result in the largest differences related to wet season and dry season start timings. The most pronounced difference is in the dry season timing, which is substantially earlier in the FFC-F. This difference then carries over to other related metrics such as spring duration and rate of change and dry season duration. The median wet season timing for both calculators is very similar, but the range of timings produced by the FFC-R is much larger and trends slightly earlier, which then carries over to wet season duration. The metrics with the largest differences between the two calculators are presented below in Figure 9.

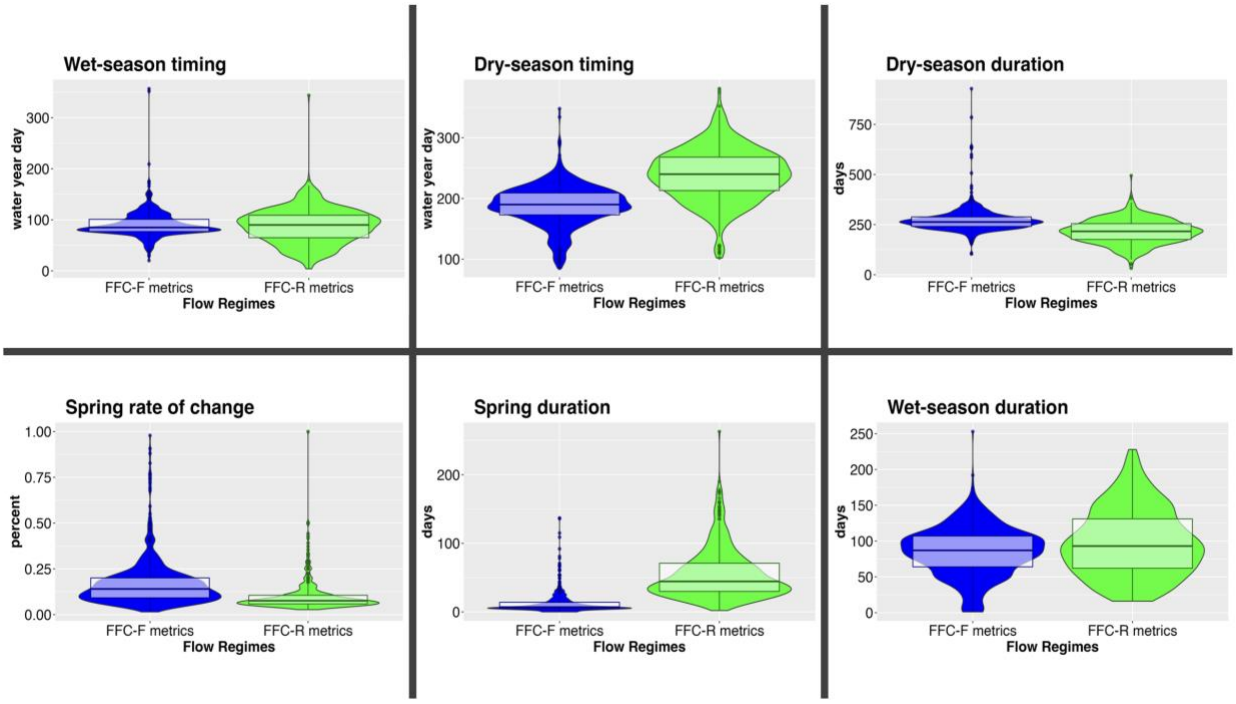

Figure 9: Metrics with significant differences between the FFC-F and FFC-R in FER Systems

A final difference between the two calculators is the number of years metrics are produced by each calculator. The FFC-F identifies 7%-10% more years with metrics than the FFC-R. This is likely due to the increased no-flow or zero-flow day threshold in the FFC-F. The FFC-F has a limit of 364 zero-flow days in a water year to run, whereas the FFC-R has a limit of 270 zero-flow days in a water year to run.

3.2.2 Highly Altered Systems

Highly altered systems vary substantially in their hydrologic pattern based on the effects of humans. Some streams are governed by dam releases for flood control and irrigation such as the large rim reservoirs around the central valley, some can be controlled by interbrain transfers for irrigation or hydropower generation such as along the Pit River in Northern California, or some are fed by mostly urban usage like the Los Angeles River. Each of these system types can have different patterns, but the FFC-F was designed to work primarily with flashy and/or flatlined systems. Although a few types of human-altered systems are listed above. There are more than just these types and no single logical ruleset can consistently identify all human-altered systems or identify the type of alterations.

To develop the FFC-F rule set and code, gages across California were run through the FFC-R and then were visually assessed to determine if they altered from the natural range of metrics and if that alteration was visually notable (i.e. rapid spring recessions in snowmelt or mixed systems, flatlined flow across the wet and dry season or stepped flow regimes). After this analysis, 17 highly altered gages were selected and used in the development of the rule set.

Comparing the metrics produced by both the FFC-R and the FFC-F for highly altered streams shows similar trends to the comparison at FER gages. One metric that diverges is the fall pulse, which matches approximately 60% of the time between the two calculators compared to 70% in the natural FES systems. Of the approximately 40% that did not match, 80% of fall pulse timings produced by the FFC-F are later than the pulses identified by the FFC-R.

The metrics with the largest difference are presented below in Figure 10.

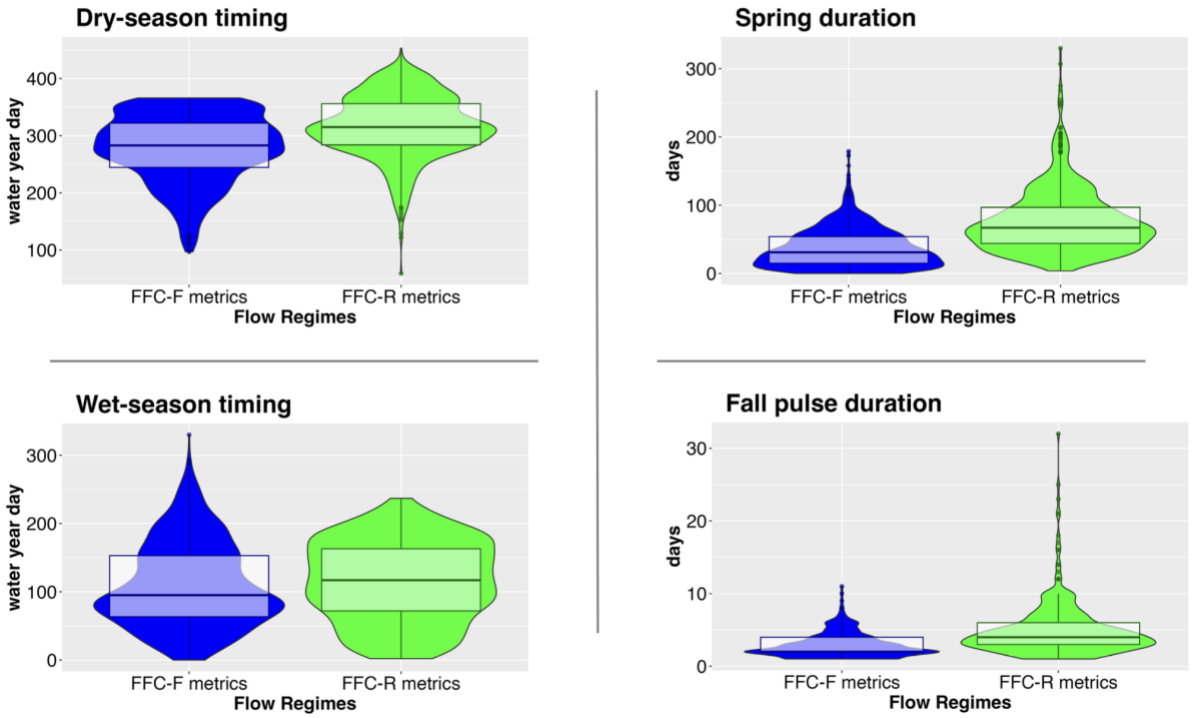

Figure 10: Metrics with significant differences between the FFC-F and FFC-R in Highly Altered Systems

The most substantial difference comparing the outputs of the two calculators is the number of metrics values they produce across years. This is most prevalent in the wet season timing where the FFC-F produced wet season start timings in approximately 30% more water years than the

FFC-R. The FFC-F also produced spring recession start timings in about 6% more water years. The two calculators produced dry season start timings for approximately the same number of water years.

4 Calculator Selection

The FFC-F was produced to calculate function flow metrics for FER streams and highly altered streams with similar characteristics. There is a relatively simple process to determine if a stream is a FER stream since every stream in California has a COMID that is related to a stream class (Lane et al. 2018). However, determining if a different stream class is altered in a reliable fashion requires a calculator selection rule set.

The FFC-R was developed first and works well for most naturalized systems where there is notable seasonality, so the FFC-R is run first before running the FFC-F, except if a stream is designated as a FER stream class. The flow data or metrics produced by the FFC-R is then used to develop rules for determining which calculator is most appropriate for the stream data.

To determine the specific decision rules, the FFC-R results and flow data were analyzed to see if there were trends in the datasets where the FFC-F worked better than FFC-R. All of the reference gages used to develop the FFC-R and a set of gages with highly altered flows known not to work well in FFC-R were assessed. Outputs from the FFC-R were compiled and then various statistical measures were produced to see if there were any measures that were markedly different in any of the flashier stream classes or the highly altered gages.

The interquartile range (IQR) of each timing metric was analyzed across gages. However, there was not an obvious trend in the groups of gages that were expected to work well with the FFC-F. Similarly, there was no notable trend in analyzing timing metrics across gages. The Hartigan Dip Test of Unimodality also did not help distinguish a threshold for which calculator to use. This is a statistical method used to assess the unimodality, or the presence of a single mode, in a dataset's distribution (Hartigan and Hartigan 1985). In many of the very flashy system and highly managed systems flows often flat line for long periods leading to more single-mode distribution of daily flows compared to more varied flow regimes in naturalized systems. However, when the analysis was run on the both the flow data and first derivative of the flow data for each gage there was not a notable trend.

The first statistical measure that produced promising results on differentiating which calculator should be used on a particular gage was the average number of not available (NA) values produced per water year by the FFC-R. The exact equation is shown below. The average number of NA's produced represents how frequently the FFC-R cannot produce metrics for a gage. However, to normalize this data, the Fall Pulse and Wet Season Peak Flow metrics were removed from the analysis since they are not present every year even in natural systems. Additionally, if there are data gaps for a gage, the FFC-R will give NAs for all metrics during missing water years, which could artificially inflate the counted total as well. In Figure 11, there is a trend that the highly altered gages average NA's IQR lower bound is around 0.7 to 0.8, which could be a good rule on when to switch to using the FFC-F.

$$Avg\ Ann.\ NAs = \frac{\left(\sum_{i=1}^{N_{WY}} \sum Metrics(excl.\ Fall\ and\ Peak)_i == NA\ \right)}{N_{WY}}$$

Where,

$Avg\ Ann.\ NAs$ is the average number of NA's produced by the FFC-R per water year,

N_{WY} is the number of water years analyzed by the FFC-R, and

$Metrics(excl.\ Fall\ and\ Peak)_i$ are all the non-fall and non-wet season peak flow related metrics.

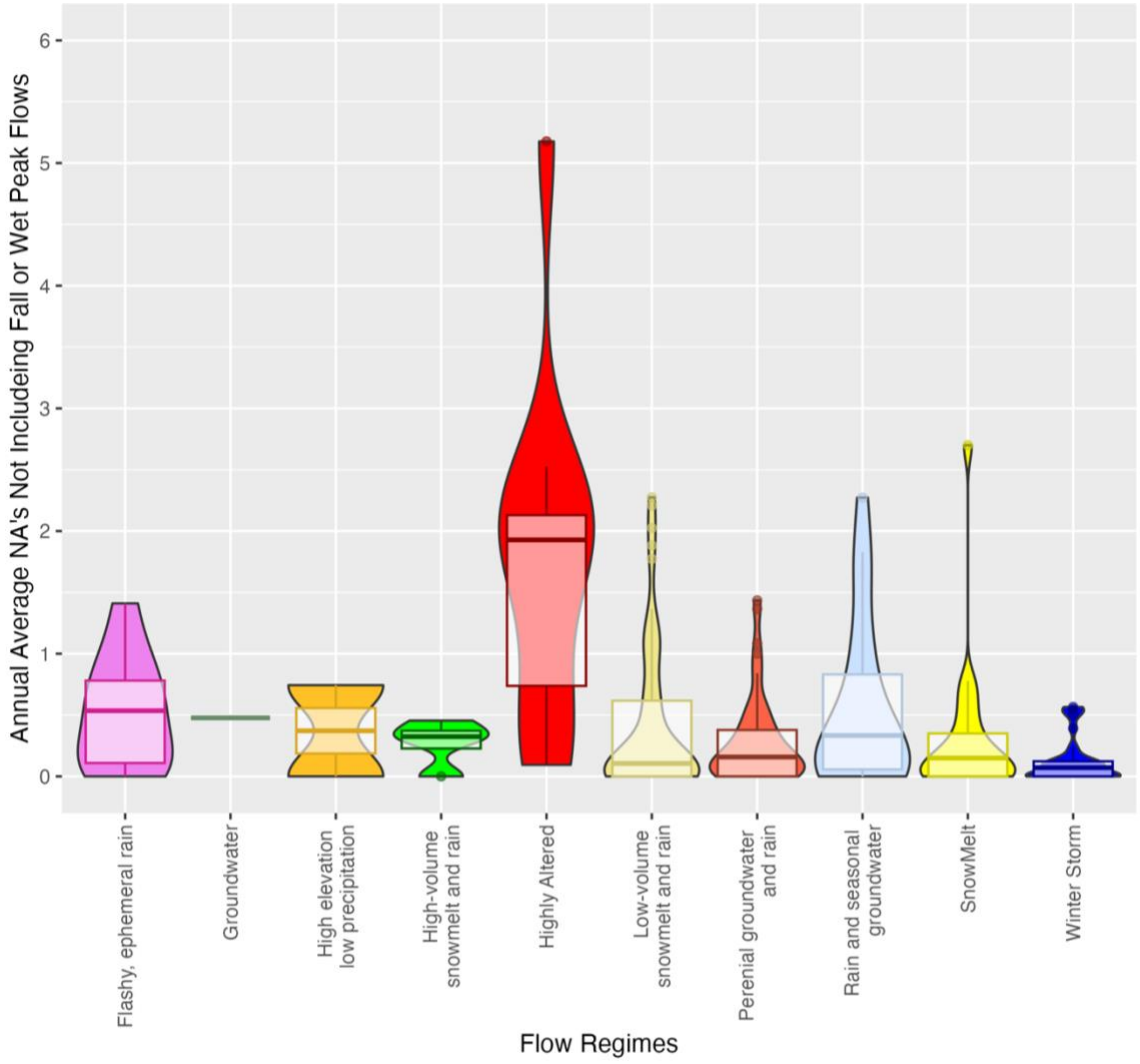

Figure 11: Average number of NA's produced by the FFC-R for each stream class reference gage and highly altered gage. There is a break in interquartile ranges of the reference gages compared to the FER gage and highly altered gages around 0.5 and 0.7.

Another promising statistical measure to differentiate which calculator should be used was the Richards-Baker Flashiness Index (RBFI). The RBFI is a metric to quantify the flashiness of a stream's flow regime. This index provides a measure of the variability in streamflow, with higher values indicating greater variability or "flashiness." Rapid changes in flow rates characterize streams with high flashiness. The RBFI is calculated using the following equation.

$$RBFI = \frac{\sum_{i=1}^{n} |q_i - q_{i-1}|}{\sum_{i=1}^{n} q_i}$$

,

where,

q is the daily flow data in cubic feet per second (cfs)

The RBFI does well at predicting if a stream is rain-driven, with all four of the classes having the highest median RBFI (Figure 12). Notably, the FER streams had the highest RBFI, which the FFC-F is designed to work well on. However, the highly altered gages, which usually perform better with the FFC-F, are generally on the lower end of the RBFI.

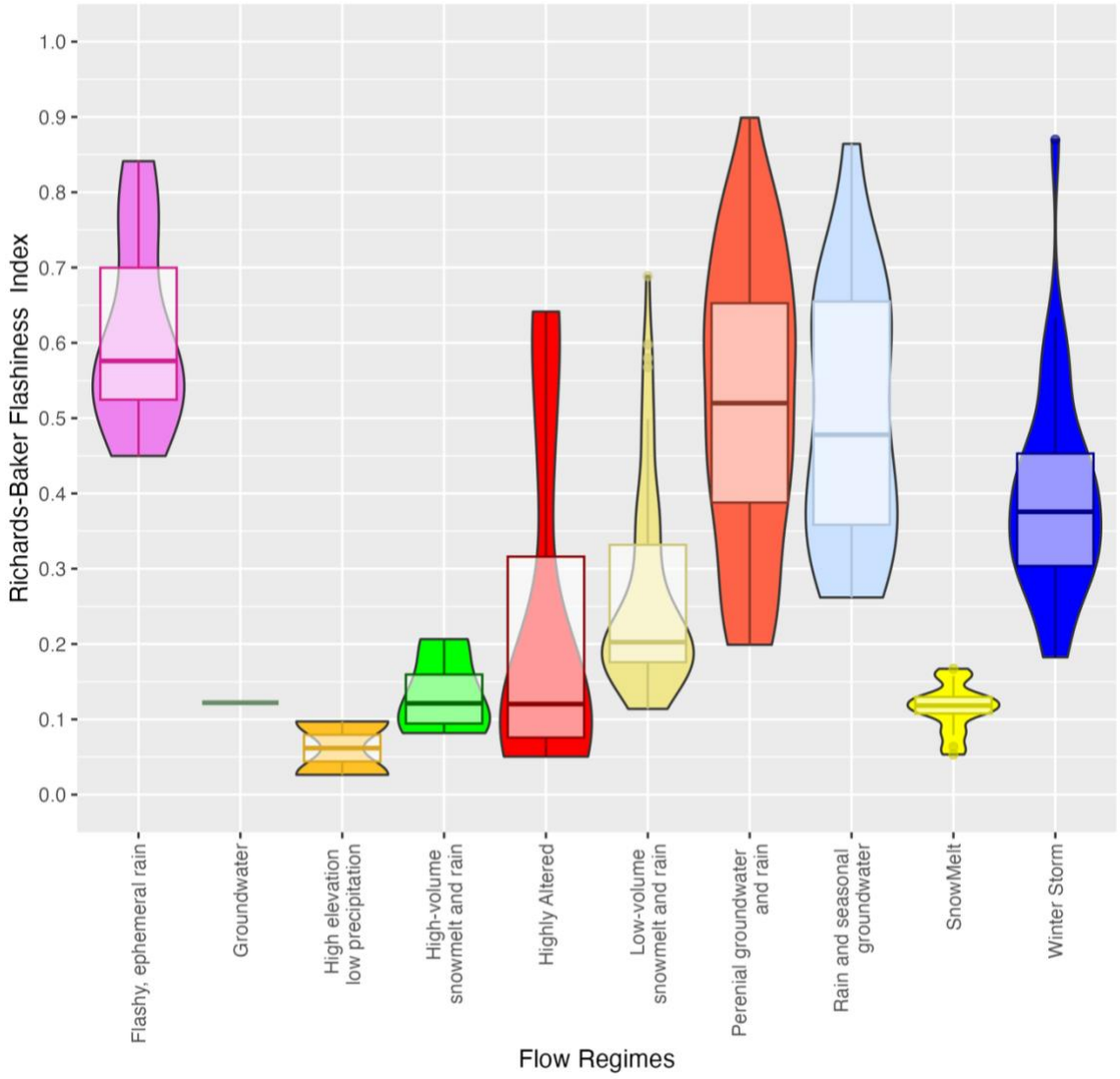

Figure 12: RBFI calculated using all flow data across stream classes and in highly altered streams.

Fortuitously the range of average annual number NA's value produced by FFC-R, generally 0-1 in reference systems, is similar in range to the RBFI ranges (0-0.9). This means that we could combine them to see if that also has a notable trend in distinguishing the FER and highly altered gages. Figure 13 shows that generally there is a good break point between IQR for the highly altered gages and the non-FER reference gages around 1.25. Additionally, there is more overlap in the IQRs of the highly altered streams and the FER streams than in other rules explored above.

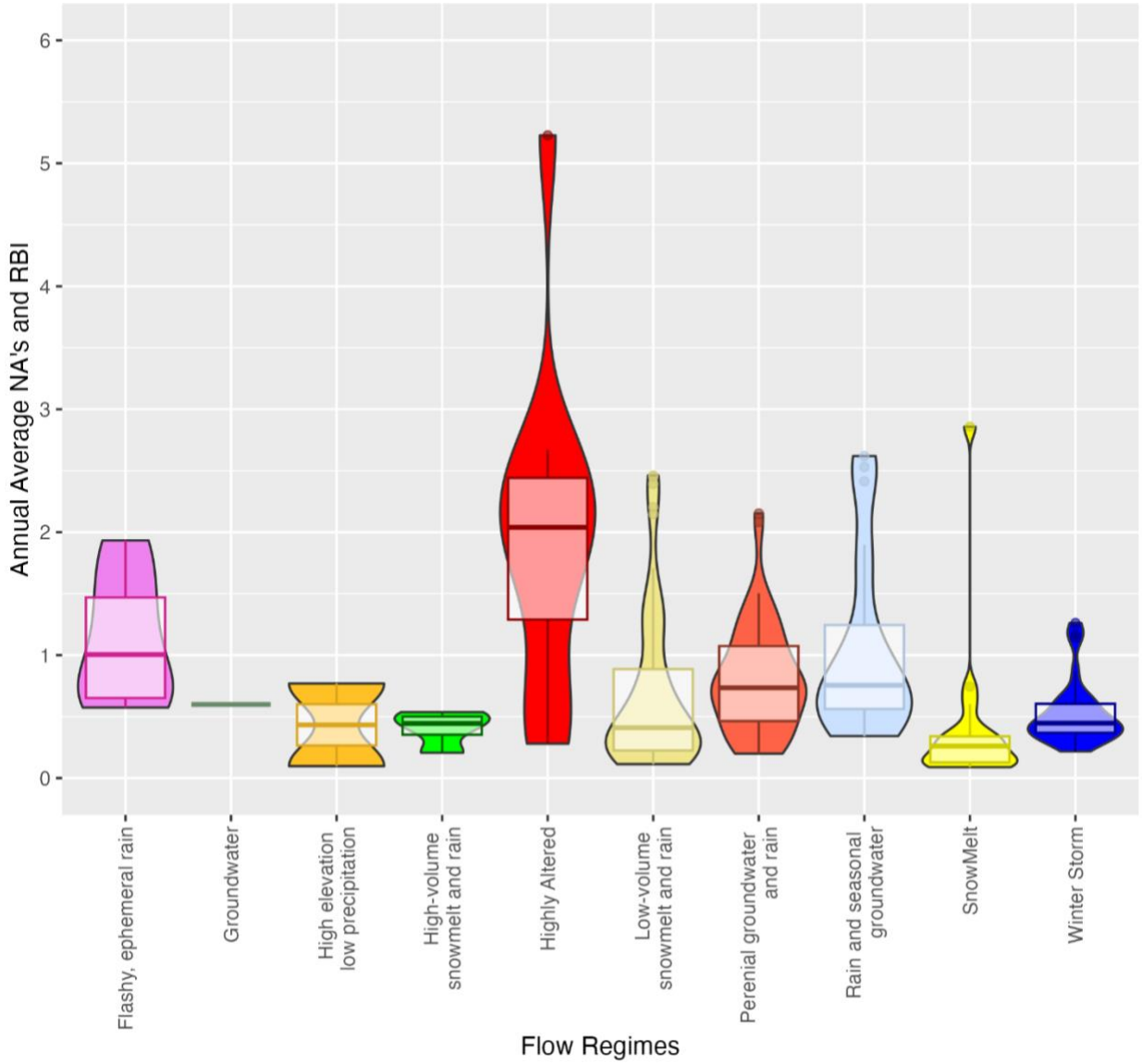

Figure 13: A Comparison of the annual average NAs produced by FFC-R summed with RBFI across stream classes.

To use the average annual number of NAs and the RFBI to determine a rule for when to use each calculator, 25 gages were selected. Twelve (12) gages were selected because they worked well with the FFC-F and thirteen (13) gages were selected because they ran better on the FFC-R. The gages used in the test were neither reference gages nor gages used to develop the FFC-F. The top

five rule sets were tested on these 25 gages to determine their potential success at predicting which calculator the flow data worked better with (Table 3).

Table 3: Calculator Rule Set Selection Testing

	Rule Set				
Success Percentage	Avg NA >1	Avg NA >0.8	Avg NA > 0.7	Avg NA + RBFI > 0.8	Avg NA + RBFI > 1
	88	88	92	92	88

To test and validate each of the top-performing calculator selection rule sets, 120 new USGS stream gages were then randomly selected from across California. Of the 120 gages only 66 gages had enough valid data to run the FFC-R (minimum of 10 water years of valid data). These 66 gages had a total of 2649 water years of data combined. The flow data for each gage along with the metrics produced by each calculator were then visually analyzed looking at which calculator performed better. Performance was analyzed subjectively by the author, generally looking for cases where one of the calculators would mis-characterize a timing as documented here and in Patterson er al. (2020). Then the rule set was tested to see if they selected the better-performing calculator. The results of validation are presented in Table 4.

Table 4: Calculator Rule Set Selection Validation

	Rule Set				
Success Percentage	Avg NA >1	Avg NA >0.8	Avg NA > 0.7	Avg NA + RBFI > 0.8	Avg NA + RBFI > 1

80.9	88.9	90.5	92.1	88.9

The results in Table 4 indicate that using either the average number of NAs over 0.7 or the average number of NAs plus the RFBI over 0.8 would select the better-performing calculator over ninety percent of the time. The stream gages used for both the testing and validation are presented in Appendix A.

5 Case Studies

The functional flow metrics produced by the FFC-R and used in CEFF have worked for many applications. However, this section highlights two example cases where the FFC-F gives more accurate information that would be important for regulation, planning, and assessment.

5.1 Sacramento River Near Keswick Dam

The Sacramento River is one of few groundwater-influenced systems in California (Lane et al. 2018). Groundwater systems generally have large drainage basins leading to high baseflows in both the wet and dry seasons. These basins are naturally very predictable, but due to large baseflows they tend to be not be highly seasonal (CEFWG 2021).

The Sacramento River is dammed by California's largest reservoir, Shasta Dam and Reservoir, which reduces flood risk and supplies water for the Central Valley Project. This damming has significantly changed the flow regime from before the dam was built. Figure 14 illustrates how flow is shifted from the winter months to the summer months when Shasta Reservoir is releasing water for irrigation and export uses.

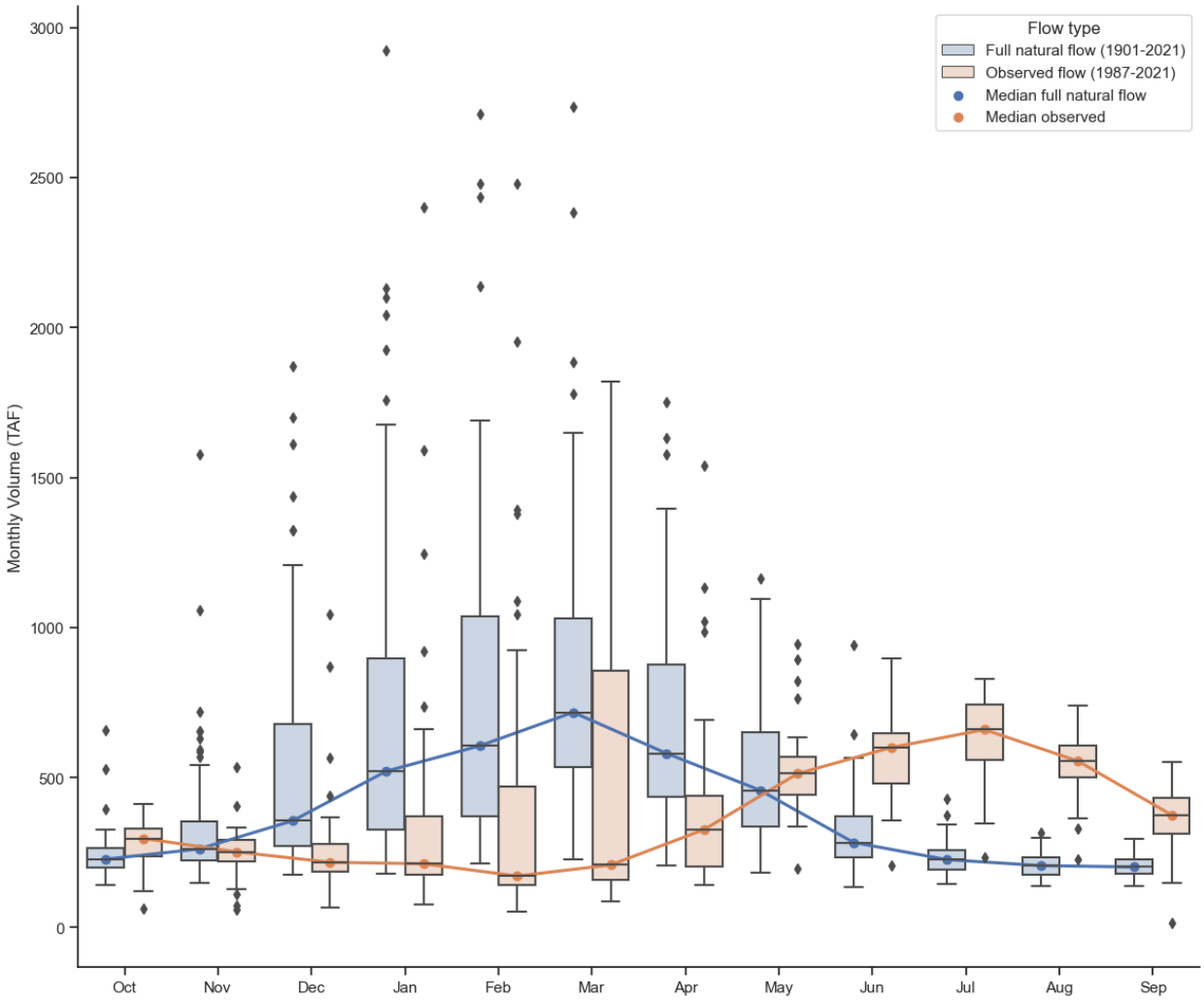

Figure 14: Monthly mean full natural flow rate (blue) and monthly mean observed flow (orange) on the Sacramento River below Shasta Dam. Full natural flow from California Data Exchange Center (CDEC) site Sacto Inflow-Shasta ('SIS') and mean observed flow from CDEC site Shasta Dam ('SHA). Box plots indicate the historical variability for each month.

Figure 14 shows the previously discussed trend where the median monthly released flows in the wet season (January-March) are roughly half the median full natural flow. In the summer (June-September) the trend is reversed with the released flow being much higher than the natural flow range. This can be seen better with a comparison daily hydrograph for the full natural flow (FNF) and the observed flow from below Keswick Dam (Figure 15).

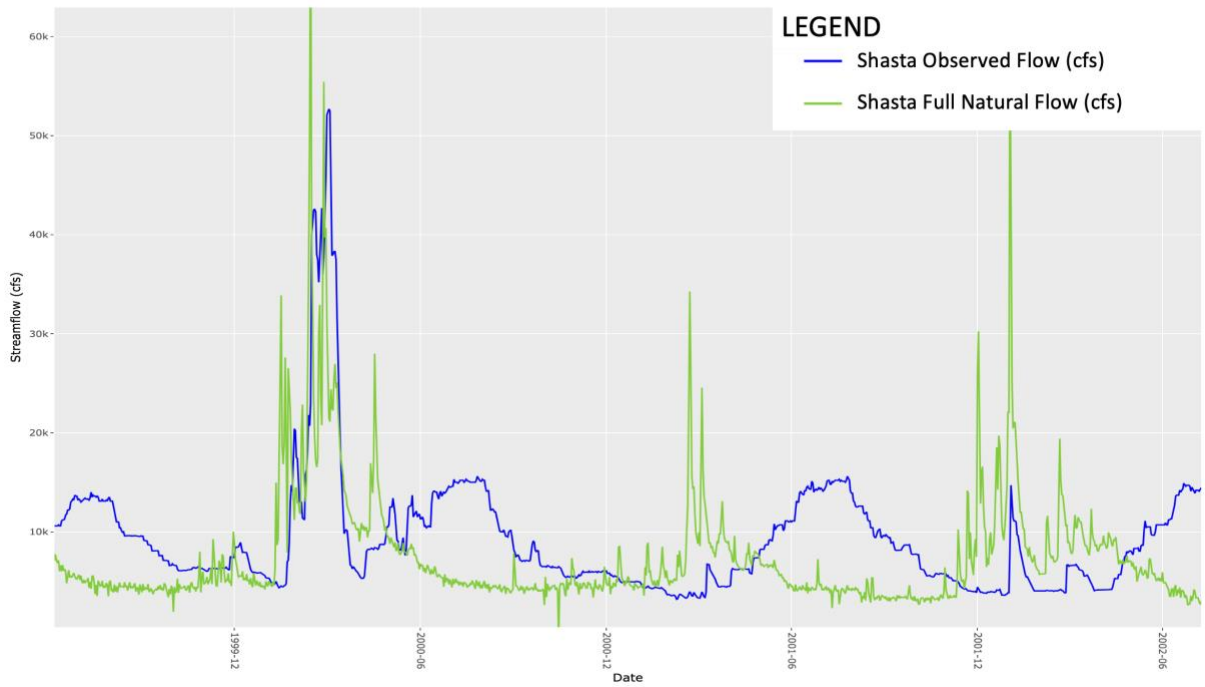

Figure 15: A comparison of FNF (green) and overserved flow (blue) in the Sacramento River around Shasta Reservoir in an above normal year (WY 2000) and a dry year (WY 2001).

In Figure 15, one can see that except when there are flood flows or spills in the reservoir during wet years, most if not all the natural flow into Shasta is stored and then released in the summer for irrigation and other anthropogenic uses. However, the metrics produced by the FFC-R show that although it identifies many of the issues we see, it misses some crucial data especially for the wet season (Figure 16).

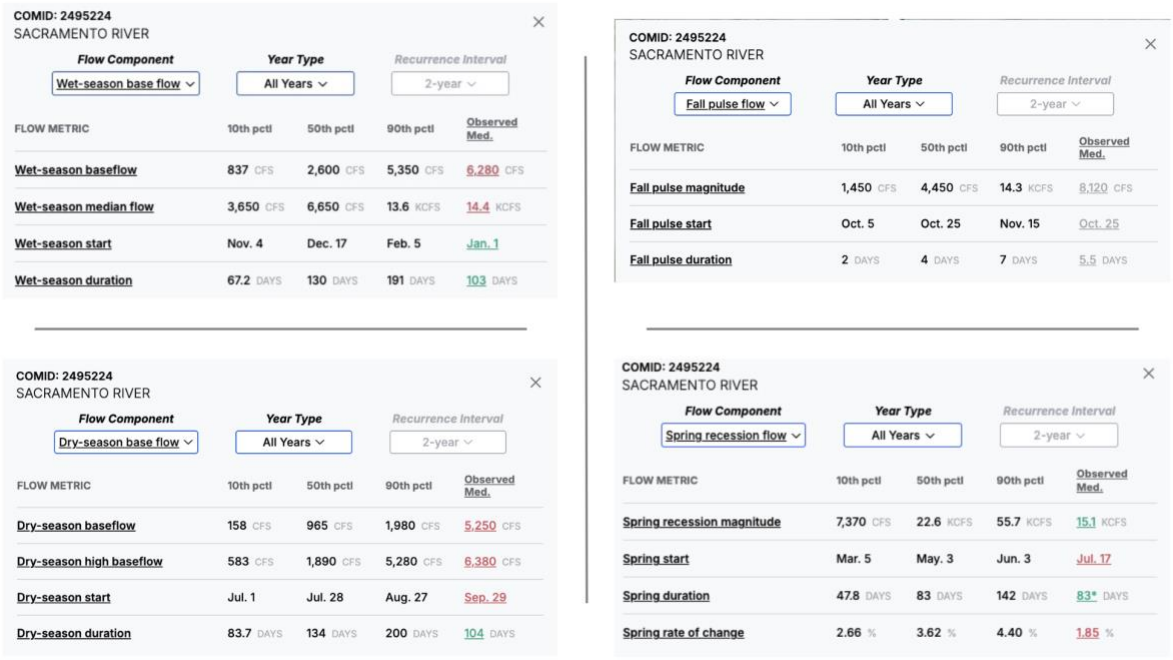

Figure 16: Natural ranges of function flow metrics for the Sacramento River below Keswick Dam compared to the observed median values (Grantham et al. 2022). Values in green are considered unaltered and values in red are considered likely altered (CEFWG 2021).

From Figure 16 and Figure 15, the FFC-R does not properly capture what is occurring for the start of the wet season and dry season duration. However, using the FFC-F, the median wet season timing is February 9th, which is outside of the IQR of the natural range and would be considered altered according to CEFF. Similarly, the median dry season duration of 216 days calculated by the FFC-F is also outside of the IQR of the natural range and would be considered altered as well. Based on more accurate results from the FFC-F, flow releases do not provide expected functional flow ranges from the natural system. Environmental flows could be designed to better fulfill some functionality of the ecosystems downstream in the Sacramento River.

5.2 Salinas River near Pozo California

Salinas River near Pozo California is a USGS stream gage, Gage ID: 11143500, located in the Santa Lucia Mountain Range approximately 14 miles east of San Luis Obispo California. This gage was a reference gage for the perennial groundwater and rain stream class from water year 1950 to 1983. This gage is located upstream of Santa Margarita Dam, which is operated by the city of San Luis Obispo through a lease with the United State Army Corps of Engineers (USACE) for water supply purposes. The gage location is located approximately 6 miles upstream of the reservoir and gages over sixty percent of the reservoir's catchment area. Based on location, flows at this gage would be expected to be similar to the natural ranges of functional flow metrics determined by Grantham et al. (Grantham et al. 2022) (Figure 17).

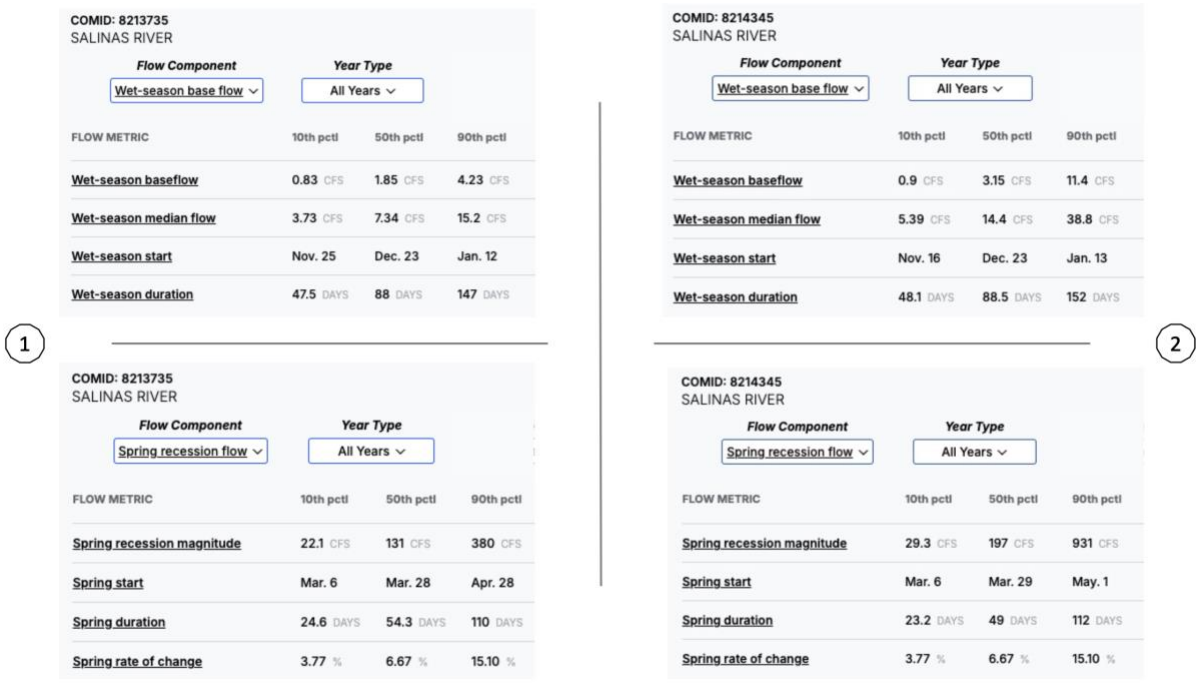

Figure 17: A comparison of the natural range of function flow metrics predicted for the reference gage 11143500 - Salinas River near Pozo California (1) and gage 11144600 - Salinas River Below Salinas Dam (2).

Although the metrics calculated by the FFC-R and FFC-F are similar, the primary differences are wet season magnitudes and spring recession start magnitude likely due to the larger catchment size at the dam site. In Figure 18, which plots metrics from each calculator on the hydrograph for two water years, one of the wet season start times appears to be too early and both the presented dry season start timings are well after the flow has flat-lined after the spring recession (Figure 18).

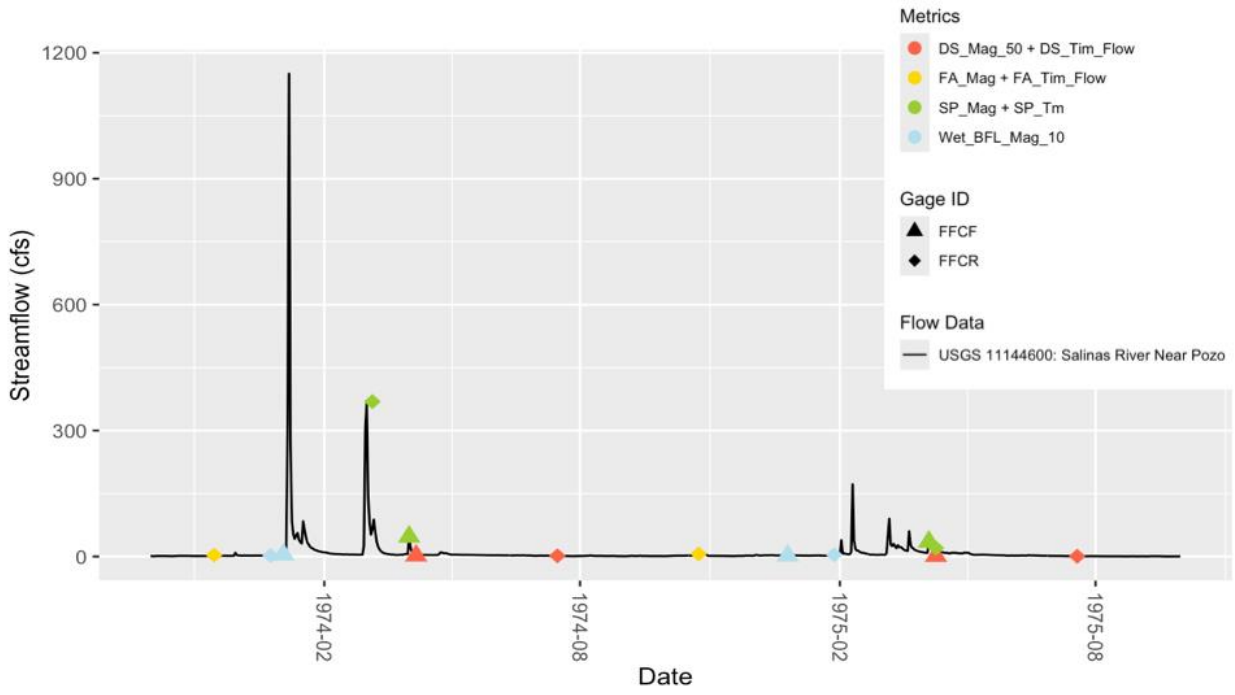

Figure 18: Functional Flow Metrics Calculated by the FFC-R for Salinas River near Pozo California. In water years 1974 and 1975, the dry season start is months after the flow has flatlined. In 1974 and 1976, the wet season start is identified while flow is still relatively flat before base flows increased.

Figure 19 compares flows above and below Salinas Dam, indicating some flow alteration perhaps due to storage of flow during storm events for later diversion to San Luis Obispo. Although there are larger peak flows in the winter months below the dam, this is to be expected in a larger watershed and is likely caused by reservoir spill events at the dam.

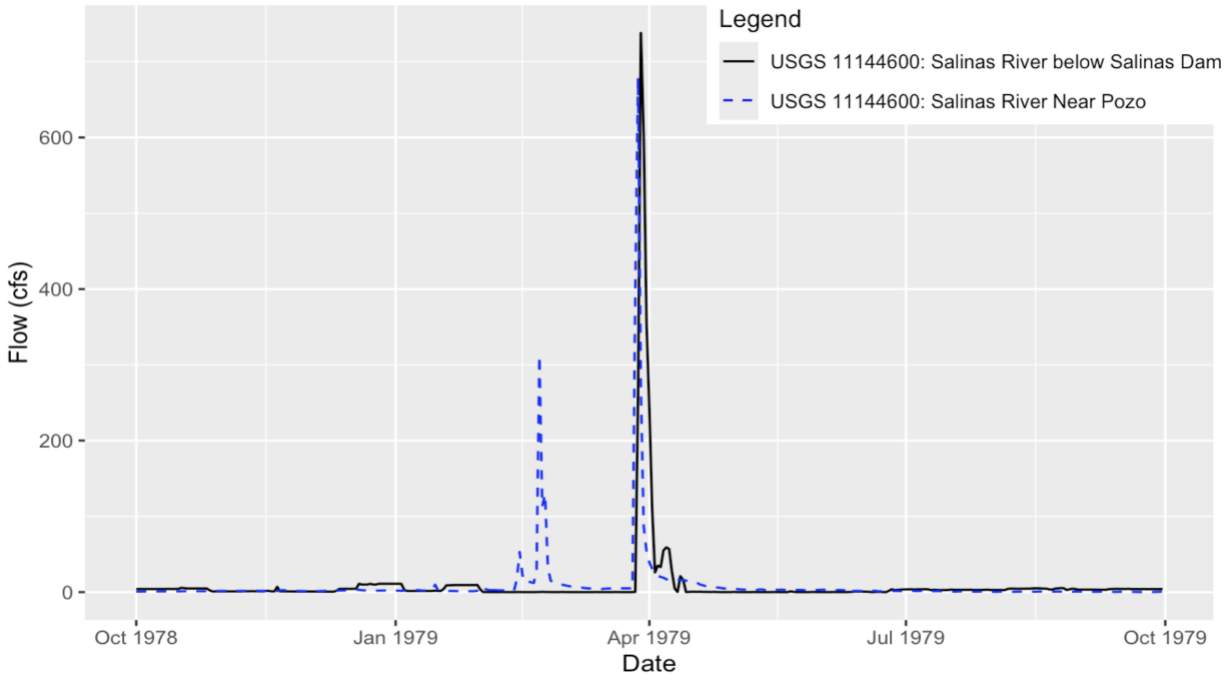

Figure 19: Comparing Flows from Reference Gage 11143500: Salinas River Near Pozo and gage 11144600: Salinas River below Salinas Dam for water year 1979.

If the City of San Luis Obispo wanted to adopt an environmental flow practice based on CEFF, they could develop flow schedules based on the natural range of functional flow metrics. An example method was presented for the Tuolumne River using bulletin 120 forecasts (Murdoch 2024). For this case study, a simpler approach was taken. Firstly, since there is no full natural flow data at the dam, the environmental flow regime was developed based on flows at the reference gage (USGS gage id: 11143500 - Salinas River near Pozo California). Additionally unlike in the Murdoch (2024) study, this flow schedule will not be adaptively produced and instead will be produced based on a particular water years total volume percentile during the time frame that the gage was considered naturalized (1950 to 1983).

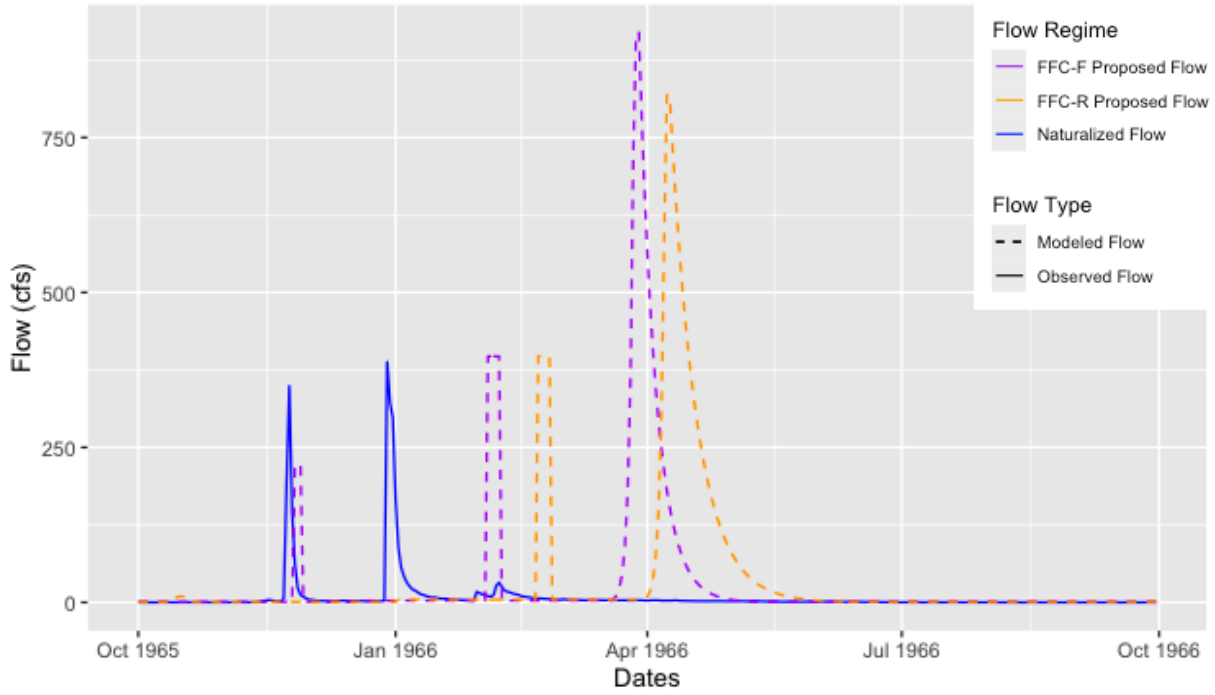

Figure 20: Comparing environmental flow regimes produced based on the FFC-F and the FFC-R and to the observed flow for Water Year 1966.

Figure 20 compares the observed flow from water year 1966 (annual volume percentile 54.55) to the flow regimes produced following the method in Murdoch (2024) for a 54.5 water year percentile. Both calculators were able to produce environmental flow regimes but did not perform well at accurately capturing the timing of the spring pulse and recession. However, the flow regime from the FFC-F metrics did more accurately capture the number of peaks that occurred during the water year and was closer to capturing the timing of the peaks.

The inaccurate size of the spring pulse and recessions shown in Figure 20 is one drawback to the method outlined in Murdoch (2024) in that a linear relationship is used to link the functional flow metrics with water year percentiles. However, in the spring magnitude relationship with annual flow percentile from both calculators here, there is a break around the 50th annual flow percentile, where the spring pulse and recession have almost no magnitude (Figure 21). Further

discussion on the limitations of how such relationships are defined is provided in Murdoch (2024).

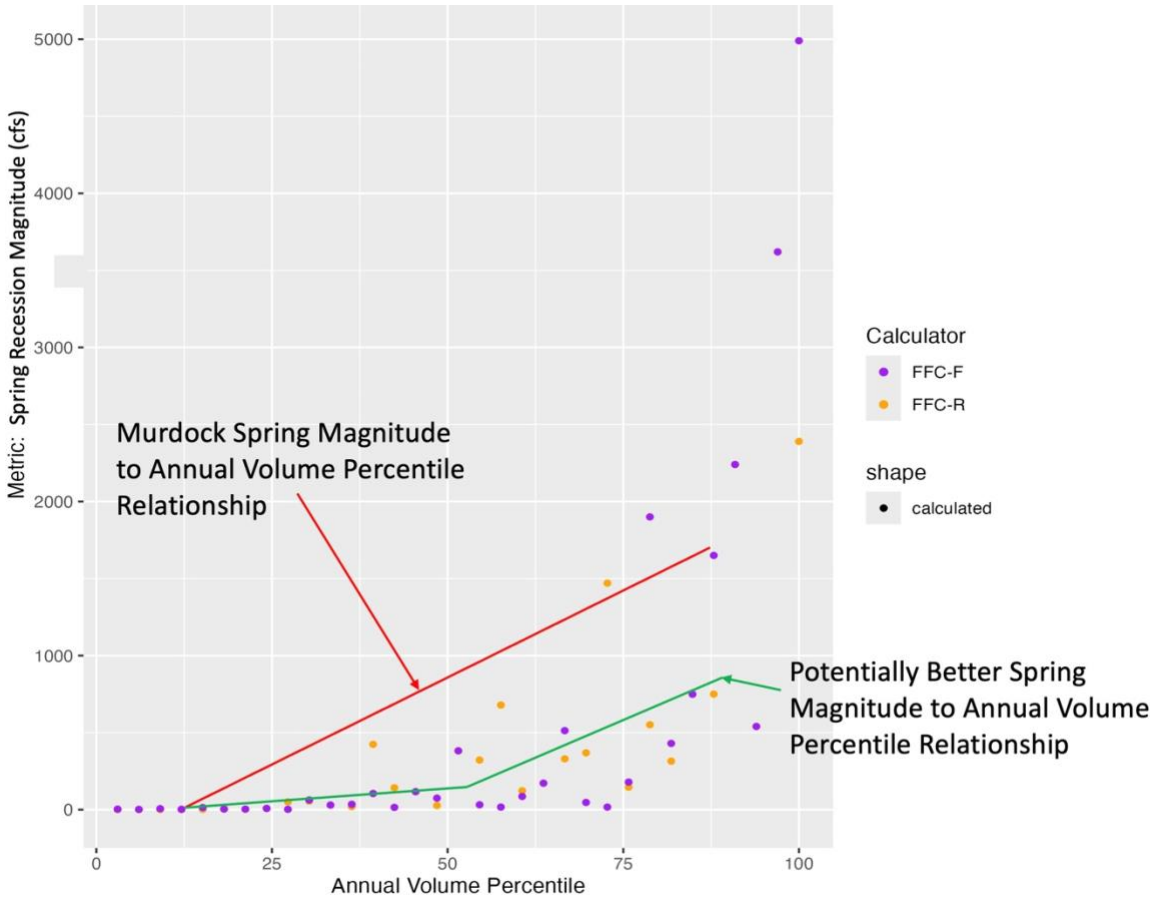

Figure 21: Functional flow metric to annual flow volume percentile relationships. The relationship in red is proposed in Murdoch 2024, and the relationship in green is a potentially more accurate piecewise function also discussed in Murdoch 2024.

6 Conclusion

CEFF presents a comprehensive approach not focused on a single species or system type. CEFF has been supported by the Functional Flow Calculator developed in 2020 for naturalized systems (FFC-R), allowing users to analyze most naturalized river systems accurately. This study presents a method to accurately predict the CEFF functional flow metrics in flashy stream

systems and altered stream systems with similar properties by removing the wide filtering used in the FFC-R and instead looking for more abrupt changes in flow to indicate seasonal change.

The product that is the outcome of this study is a publicly available code package (https://github.com/camcarpenter6/Alternate-Ruleset-FFC-BETA) that accurately calculates metrics in 95% of water years. This work will assist users in accurately assessing their current operating conditions from a functional flows perspective with metrics that can be compared to the natural ranges developed in Granthem et al. 2022. This tool can also then be applied to developing new environmental flow regimes, in regulatory processes like FERC relicensing, where the flow regimes may be closer to following the metrics recommended by CEFF but do not closely follow natural stream variability or gradual seasonal changes in flow patterns. These flow regimes will likely be better analyzed using the FFC-F instead of the FFC-R.

The FFC-F and rule set developed here do have limitations. It produces less accurate metrics in non-flashy naturalized systems than the FFC-R. Additionally, both the FFC-F and FFC-R do not perform well in stream systems with flow schedules designed for irrigation, where water is stored in the winter (the natural wet season) to be released during the summer inverting the natural hydrograph. This causes an issue since both calculators are designed to evaluate a single water year. These inverted hydrographs frequently have a “spring recession” cross into the following water causing either inaccurate metrics or the inability for metrics to be produced altogether. Developing a tool that can better analyze these types of systems could help with understanding system impairment without visual comparison.

Uncertainty about the future of water supply in California due to climate change and an already over-allocated system, requires water managers, regulators, and dam operators to reimagine how the design of environmental flow regimes. The FFC-F in conjunction with CEFF provides a valuable tool for stakeholders to evaluate current operating conditions and plan more functional flow regimes to protect the native and endemic species of California.

7 References

Arthington, Angela H., Jonathan G. Kennen, Eric D. Stein, and J. Angus Webb. 2018. "Recent Advances in Environmental Flows Science and Water Management—Innovation in the Anthropocene." *Freshwater Biology* 63 (8): 1022–34. https://doi.org/10.1111/fwb.13108.

Baruch, Ethan, Sarah M. Yarnell, Theodore Grantham, Jessica Ayers, Andrew Rypel, and Rob A. Lusardi. In Review. "Mimicking Functional Elements of the Natural Flow Regime Promotes Native Fish Recovery in a Regulated River." *Ecology Applications*.

"Bulletin_15_1967.Pdf." n.d. Accessed January 3, 2024. https://water.usgs.gov/osw/bulletin17b/Bulletin_15_1967.pdf.

"California Environmental Flows Framework." n.d. Accessed July 12, 2023. https://ceff.ucdavis.edu/sites/g/files/dgvnsk5566/files/media/documents/CEFF%20Technical%20Report%20Ver%201.0%20Mar_31_2021_DRAFT_FINAL%20for%20web.pdf.

United States Geological Survey (USGS). 1982. "Guidelines For Determining Flood Flow Frequency". *Bulletin #17B of the Hydrology Subcommittee*. Accessed January 3, 2024. https://water.usgs.gov/osw/bulletin17b/dl_flow.pdf.

Freeman, Mary C., Zachary H. Bowen, Ken D. Bovee, and Elise R. Irwin. 2001. "Flow and Habitat Effects on Juvenile Fish Abundance in Natural and Altered Flow Regimes." *Ecological Applications* 11 (1): 179–90. https://doi.org/10.2307/3061065.

Gasith, Avital, and Vincent H. Resh. 1999. "Streams in Mediterranean Climate Regions: Abiotic Influences and Biotic Responses to Predictable Seasonal Events." *Annual Review of Ecology, Evolution, and Systematics* 30 (Volume 30, 1999): 51–81. https://doi.org/10.1146/annurev.ecolsys.30.1.51.

Grantham, Theodore E., Daren M. Carlisle, Jeanette Howard, Belize Lane, Robert Lusardi, Alyssa Obester, Samuel Sandoval-Solis, et al. 2022. "Modeling Functional Flows in

California's Rivers." *Frontiers in Environmental Science* 10 (March). https://doi.org/10.3389/fenvs.2022.787473.

Hartigan, J. A., and P. M. Hartigan. 1985. "The Dip Test of Unimodality." *The Annals of Statistics* 13 (1): 70–84. https://doi.org/10.1214/aos/1176346577.

Hassan, Marwan, Roey Egozi, and Gary Parker. 2006. "Experiments on the Effect of Hydrograph Characteristics on Vertical Grain Sorting in Gravel Bed Rivers." *Water Resources Research - WATER RESOUR RES* 420 (September). https://doi.org/10.1029/2005WR004707.

Lambeets, Kevin, Martijn L. Vandegehuchte, Jean-Pierre Maelfait, and Dries Bonte. 2008. "Understanding the Impact of Flooding on Trait-Displacements and Shifts in Assemblage Structure of Predatory Arthropods on River Banks." *Journal of Animal Ecology* 77 (6): 1162–74. https://doi.org/10.1111/j.1365-2656.2008.01443.x.

Lane, Belize A., Samuel Sandoval-Solis, Eric D. Stein, Sarah M. Yarnell, Gregory B. Pasternack, and Helen E. Dahlke. 2018. "Beyond Metrics? The Role of Hydrologic Baseline Archetypes in Environmental Water Management." *Environmental Management* 62 (4): 678–93. https://doi.org/10.1007/s00267-018-1077-7.

Lee, Pey-Yi, and Jian-Ping Suen. 2012. "Niche Partitioning of Fish Assemblages in a Mountain Stream with Frequent Natural Disturbances – an Examination of Microhabitat in Riffle Areas." *Ecology of Freshwater Fish* 21 (2): 255–65. https://doi.org/10.1111/j.1600-0633.2011.00544.x.

Lytle, David A., and David M. Merritt. 2004. "HYDROLOGIC REGIMES AND RIPARIAN FORESTS: A STRUCTURED POPULATION MODEL FOR COTTONWOOD." *Ecology* 85 (9): 2493–2503. https://doi.org/10.1890/04-0282.

Madej, Mary Ann. 1999. “Temporal and Spatial Variability in Thalweg Profiles of a Gravel-Bed River.” *Earth Surface Processes and Landforms* 24 (12): 1153–69. https://doi.org/10.1002/(SICI)1096-9837(199911)24:12<1153::AID-ESP41>3.0.CO;2-8.

Murdoch, Lindsay E. 2024. “Adaptively Operating a Fixed-Percent Environmental Flow Budget with a Functional Flows Approach.” Davis, California: University of California, Davis.

Opperman, Jeffery J, Peter B. Moyle, Eric W. Larsen, Joan L. Florsheim, and Amber D. Manfree. 2018. “Floodplains: Processes and Management for Ecosystem Services.” *Hungarian Geographical Bulletin* 67 (June):189–90. https://doi.org/10.15201/hungeobull.67.2.6.

Patterson, Noelle K., Belize A. Lane, Samuel Sandoval-Solis, Gregory B. Pasternack, Sarah M. Yarnell, and Yexuan Qiu. 2020. “A Hydrologic Feature Detection Algorithm to Quantify Seasonal Components of Flow Regimes.” *Journal of Hydrology* 585 (June):124787. https://doi.org/10.1016/j.jhydrol.2020.124787.

Petts, Geoff, and Angela Gurnell. 2013. “Hydrogeomorphic Effects of Reservoirs, Dams, and Diversions.” *Treatise on Geomorphology* 13 (March):96–114. https://doi.org/10.1016/B978-0-12-374739-6.00345-6.

Poff, N. LeRoy, J. David Allan, Mark B. Bain, James R. Karr, Karen L. Prestegaard, Brian D. Richter, Richard E. Sparks, and Julie C. Stromberg. 1997. “The Natural Flow Regime.” *BioScience* 47 (11): 769–84. https://doi.org/10.2307/1313099.

Postel, S, and B Richter. 2015. “Rivers for Life: Managing Water for People and Nature.” Island Press. July 9, 2015. https://islandpress.org/books/rivers-life.

Shafroth, Patrick B., Gregor T. Auble, Juliet C. Stromberg, and Duncan T. Patten. 1998. “Establishment of Woody Riparian Vegetation in Relation to Annual Patterns of

Streamflow, Bill Williams River, Arizona." *Wetlands* 18 (4): 577–90. https://doi.org/10.1007/BF03161674.

Tharme, R. 2003. "A Global Perspective on Environmental Flow Assessment: Emerging Trends in the Development and Application of Environmental Flow Methodologies for Rivers." *RIVER RESEARCH AND APPLICATIONS* 19 (5–6): 375–681. https://doi.org/10.1002/rra.736.

Ward, J. V. 1998. "Riverine Landscapes: Biodiversity Patterns, Disturbance Regimes, and Aquatic Conservation." *Biological Conservation*, Conservation Biology and Biodiversity Strategies, 83 (3): 269–78. https://doi.org/10.1016/S0006-3207(97)00083-9.

Williams, John, Peter B. Moyle, J. Angus Webb, and G. Mathias Kondolf. 2019. *Environmental Flow Assessment: Methods and Applications*. https://onlinelibrary.wiley.com/doi/epub/10.1002/9781119217374.

Yarnell, Sarah M., Geoffrey E. Petts, John C. Schmidt, Alison A. Whipple, Erin E. Beller, Clifford N. Dahm, Peter Goodwin, and Joshua H. Viers. 2015. "Functional Flows in Modified Riverscapes: Hydrographs, Habitats and Opportunities." *BioScience* 65 (10): 963–72. https://doi.org/10.1093/biosci/biv102.

Yarnell, Sarah M., Eric D. Stein, J. Angus Webb, Theodore Grantham, Rob A. Lusardi, Julie Zimmerman, Ryan A. Peek, Belize A. Lane, Jeanette Howard, and Samuel Sandoval-Solis. 2020. "A Functional Flows Approach to Selecting Ecologically Relevant Flow Metrics for Environmental Flow Applications." *River Research and Applications* 36 (2): 318–24. https://doi.org/10.1002/rra.3575.

Appendix A: Gage Data

Functional Flow Calculator – Flashy Development Gages: Class 7 Reference Gages

USGS Gage ID	COMID	Stream Class	Period of Record (Reference gage range)
11116000	17586460	7	55 (1955-1983)
11120510	17595405	7	30 (1970-1980)
11120520	17596097	7	54 (1970-2013)
11120550	17594763	7	20 (1966-1986)
11132500	17609017	7	83 (1950-1987)
11138500	17625379	7	95 (1950-2014)
11172100	17694079	7	16 (1961-1987)
11172945	2809681	7	30 (1994-2014)
11173200	2809859	7	56 (1968-2014)
11176400	2806807	7	61 (1963-2015)
11224500	14883269	7	79 (1950-2014)
11253310	14882615	7	58 (1966-2014)

Functional Flow Calculator – Flashy Development Gages: Highly Altered Gages

USGS Gage ID	COMID	Stream Class	Period of Record (Reference gage range)
10344500	8933684	3	113
10340500	8933736	3	82 (1950-1983)
10289500	8915933	1	71
10293000	8915857	1	103
10338700	8933890	3	31
10344505	8933706	3	22
11293200	343235	3	49

11292860	343265	3	38
11292900	343203	3	67
11109375	17569367	6	43
11014000	20334508	8	36
11378800	12068268	8	23
11109000	17575785	6	97
11051501	22558244	3	111
11097000	22515762	6	36
11445500	14982092	3	44 (1951-1965)
11128250	17607945	6	54

Functional Flow Calculator – Flashy: Selection Testing Gages

USGS Gage ID	COMID	Stream Class	Period of Record
11481500	8319319	4	32
11523200	8242324	3	36
11478500	2705701	4	36
11447360	15022679	4	29
11446500	948021150	2	37
11335000	20192498	8	41
11264500	21609533	1	36
11255500	19780249	7	36
11253310	14882615	7	36
11189500	14961121	1	36
11173575	2806865	7	25
11173510	2806979	7	29
11173500	2807009	7	22
11149900	8210533	6	38
11143200	17600477	6	36
11143000	8189809	6	36
11097000	22515762	6	36
11055800	22555756	3	36
10343500	8933522	3	37
11274500	2828012	6	36
11475000	2706571	4	36
11519500	3798909	3	36
11413000	8058675	3	37

11251000	19791955	2	36
11070500	22534666	8	36

Functional Flow Calculator – Flashy: Selection Validation Gages

Stream Class 0 indicates that the COMID didn't have a stream class from a previous GIS analysis.

USGS Gage ID	COMID	Stream Class	Period of Record
11090200	22525749	8	50
11528400	8232828	3	9
11454100	15039505	4	9
11023250	20331142	8	10
11246530	17116245	0	25
11144600	8214345	6	13
11362945	7948302	3	30
11352000	7926519	9	50
11042700	22545337	8	17
11425415	948021109	0	30
11521500	4440524	3	50
10260950	22660257	3	50
11526000	8245876	5	8
11234500	17114909	3	49
11482125	8316253	4	12
11289650	2823750	2	50
11181330	2803723	0	13
11417000	8063831	3	30
11104000	20365153	8	40
11057000	22557960	8	50
11295910	347255	1	8
11414360	8063671	0	30
11369000	7963509	3	33
11390000	1680009	8	50
11133000	948060325	6	60
11460920	3879992	8	12
11306000	17067108	8	28
11120530	17595369	8	20
11525854	8245896	5	20
10251300	20247268	7	60

11421720	15014349	0	24
11053000	22556090	3	20
11238400	17115579	0	43
11106400	17564046	8	9
11423500	15013993	8	20
11238500	17116205	1	80
11299500	348435	2	35
11230200	17118415	1	30
11373200	2763434	8	8
11482200	8316133	4	11
11465390	8272685	6	15
11389720	2770060	3	30
103087889	8922717	0	21
11253310	14882615	7	55
10287145	20286396	0	30
11396000	8037505	3	90
11343500	948020259	9	30
11059000	22556064	7	20
11057500	22557960	8	70
11062400	24843814	3	50
11433100	14993021	3	30
11428300	14993077	1	50
11463000	8271445	6	70
11217000	22048113	1	60
11108000	17574541	6	75
11075740	22527369	8	12
11426120	14991657	0	8
11135500	163864377	6	19
11120520	17596097	7	50
11022480	20331402	8	70
10260776	22680612	3	20
11167000	17694425	6	28
11101500	22515018	8	50
11160020	17682178	6	24
11490500	8265322	9	39
11261000	948040356	8	28
11185500	14972873	1	102
11084500	22524697	8	60
11162540	17688327	6	12

11211785	17142690	6	8
11277000	17082171	1	45
11426500	14992951	3	30
11212000	17142458	6	40
11434000	14996683	2	24
11292500	347487	1	44
11210000	14922513	3	13
11056200	22556176	3	24
11186001	14971723	1	100
10260780	22660065	0	19
11120600	17593507	4	17
11472900	8294911	3	40
11238100	17115511	0	40
11160070	17682322	6	16
11416100	8063929	0	60
10256000	948100222	3	20
11122010	17610919	7	32
10259100	22593529	8	34